CRISTIANE FRANCISCA BARBOSA

BIOCHAR-BASED PHOSPHATE FERTILIZERS: solid phase speciation and phosphorus solubility and potential as a support material for nitrogen

LAVRAS – MG

2021

CRISTIANE FRANCISCA BARBOSA

BIOCHAR-BASED PHOSPHATE FERTILIZERS: solid phase speciation and phosphorus solubility and potential as a support material for nitrogen

Thesis presented to the Federal University of Lavras, as part of the requirements of the graduate program in Soil Science, area of concentration in Soil Fertility and Plant Nutrition, to earn the title of Doctor.

Prof. Dr. Leônidas Carrijo Azevedo Melo

Advisor

LAVRAS-MG

2021

Ficha catalográfica elaborada pelo Sistema de Geração de Ficha Catalográfica da Biblioteca Universitária da UFLA, com dados informados pelo(a) próprio(a) autor(a).

Barbosa, Cristiane Francisca.
Biochar-based Phosphate Fertilizers: : Solid-phase speciation and phosphorus solubility and potential as a support material for nitrogen / Cristiane Francisca Barbosa. - 2021.
79 p.

Orientador(a): Leônidas Carrijo Azevedo Melo.

Tese (doutorado) - Universidade Federal de Lavras, 2021.
Bibliografia.

1. Biochar-based fertilizers. 2. Phosphorus speciation. 3. Nitrogen. I. Melo, Leônidas Carrijo Azevedo. II. Título.

CRISTIANE FRANCISCA BARBOSA

BIOCHAR-BASED PHOSPHATE FERTILIZERS: solid phase speciation and phosphorus solubility and potential as a support material for nitrogen

Thesis presented to the Federal University of Lavras, as part of the requirements of the graduate program in Soil Science, area of concentration in Soil Fertility and Plant Nutrition, to earn the title of Doctor.

APPROVED in May 31 2021.

Dr. Guilherme Lopes	UFLA
Dr. Luiz Arnaldo Fernandes	UFMG
Dr. Matheus Sampaio Carneiro Barreto	UM6P
Dr. Wedisson Oliveira Santos	UFU

Dr. Leônidas Carrijo Azevedo Melo

(Advisor)

LAVRAS – MG

2021

Aos meus pais, José Elton e Marinalva, as minhas irmãs Má e Paula, a minha afilhada Lavínia e á meu marido Breno.

Dedico

AGRADECIMENTOS

Dedico este trabalho em primeiro lugar a Deus por ter iluminado o meu caminho, por me dar saúde e forças para superar todos os momentos difíceis a que eu me deparei.

Aos meus pais, José Elton e Marinalva por todo amor, pelos ensinamentos, incentivo e por acreditarem em mim. Agradeço, também, aos amores da minha vida as minhas irmãs Má e Paula pela compreensão da minha ausência, companheirismo e amizade.

Ao meu companheiro, amigo e marido Breno, pelo amor, paciência, motivação, conselhos e apoio. Obrigada por caminhar comigo e fazer parte da minha jornada nesse plano.

Ao Programa de Pós-Graduação em Ciência do Solo e ao Departamento de Ciência do Solo (DCS) da Universidade Federal de Lavras (UFLA) pela oportunidade para realizar o doutorado.

O presente trabalho foi realizado com apoio do Conselho Nacional de Desenvolvimento Científico e Tecnológico (CNPq), agradeço pela concessão da bolsa de doutorado. Agradeço também à Coordenação de Aperfeiçoamento de Pessoal de Nível Superior (CAPES) e à Fundação de Apoio à Pesquisa de Minas Gerais (FAPEMIG) pelo subsídio financeiro.

Ao meu orientador professor/pesquisador Leônidas Melo, pela orientação, conselhos, confiança, paciência, sabedoria, generosidade e exemplo profissional.

Ao professor/pesquisador Alfredo Scheid Lopes (DCS/UFLA), pela amizade, conversas motivacionais e valiosas contribuições para o meu crescimento pessoal.

A todo corpo docente do DCS-UFLA por todos os ensinamentos dentro e fora da sala de aula. Ao corpo técnico do DCS/UFLA, principalmente à Mari, Lívia, Geila, Aline e Dirce pela amizade e contribuição para conclusão deste trabalho de tese.

Aos membros da banca examinadora, composta Dr. Guilherme Lopes, Dr. Wedisson Santos, Dr. Luiz Arnaldo Fernandes, Dr. Matheus Barreto e Dr. Leônidas Melo pela disponibilidade para participar e pelas contribuições na avaliação deste trabalho de tese.

A todos os membros e ex-membros do grupo GETAFS em especial ao Ferreira, Jefferson, Bárbara, Evanise e Dehon. Agradeço também, os colegas e amigos do DCS Sol, Flávia, Franklin, Fábio, Mariana, Fernanda, Sara e Monna.

Agradeço ao professor Renato Ribeiro Passos pelo auxilio na produção do biocarvão e ao professor Dean Hesterberg por toda ajuda na interpretação dos dados XANES e na melhoria do nosso trabalho.

Aos amigos da “Colônia da Esperança” em especial à Andrea pelo apoio incondicional, pela palavra sábia, pelo sorriso amigo, pelo abraço reconfortante, eu te agradeço.

De modo geral, agradeço a todos e peço desculpas àqueles cujo nomes não citei, pois não são menos importantes. Enfim, a todos que, direta e indiretamente, contribuíram para a conclusão desta caminhada.

EPÍGRAFE

Tudo tem seu apogeu e seu declinío [...]
É natural que seja assim, todavia,
quando tudo parece convergir para o que
supomos o nada, eis que a vida ressurge,
triunfante e bela!.....Novas folhas, novas flores,
na infinita benção do recomeço.
Chico Xavier

RESUMO GERAL

A associação de matéria orgânica a fontes inorgânicas de P, para obtenção de fertilizantes à base de biochar (BBFs), tem sido sugerida para aumentar a eficiência de uso do P em solos tropicais ácidos e, adicionalmente, podem aumentar a eficiência de uso de N. Apesar da resposta da cultura a fertilização com BBFs já tenha sido investigada, é imperativo compreender as formas de P no fertilizante e as transformações de tais formas de P no solo após a fertilização. Com isso, superfosfato triplo (TSP) com e sem adição de MgO, e ácido fosfórico (H_3PO_4) com MgO foram pirolisados com cama de frango (PLB) para produzir fertilizantes fosfatados à base de biochar. Com o objetivo de avaliar a eficiência agronômica dos BBFs (PLB-TSP, PLB-TSP-Mg, PLB-H_3PO_4-Mg) em relação ao TSP e um fertilizante organomineral (OMF), foi conduzido um experimento em casa de vegetação com o cultivo de mudas de café por sete meses em Latossolo Argiloso. Os BBFs originais e as amostras de solo coletadas após o crescimento do cafeeiro foram analisados para P por fracionamento químico convencional e por especiação de absorção de raios-X perto da estrutura de borda (XANES). Os BBFs com MgO aumentaram a eficiência de uso do P em cafeeiros quando comparados com TSP e OMF. Os resultados do fracionamento sequencial em BBFs confirmaram a dominância do P associado ao Ca e ao Mg em compostos de baixa solubilidade, como a monetita e o pirofosfato identificados por XANES. Houve aumento das frações lábil e moderadamente lábil de P após o cultivo com PLB-TSP-Mg e PLB-H_3PO_4-Mg. Os resultados confirmam que os BBFs podem aumentar a eficiência de uso do P em um Latossolo no médio a longo prazo e promover um maior efeito residual da fertilização devido à presença de compostos orgânicos de maior estabilidade. Os BBFs também apresentam propriedades favoráveis para aumentar a eficiência de uso de N ao mesmo tempo que fornece P para as plantas. Nesse sentido, um segundo estudo foi realizado no qual PLB-H_3PO_4-Mg foi enriquecido com ureia na proporção 4:5 (BBF:ureia, p/p) com o objetivo de gerar um fertilizante 15-15 % NP de liberação lenta (PLB-N) para ser usado em uma única aplicação no solo. PLB-N foi caracterizado por pH, CE, conteúdo de nutrientes e solubilidade de P e analisado por microscopia eletrônica de varredura (MEV) e espectroscopia de energia dispersiva de raios-X (EDX). Foi conduzido um experimento em casa de vegetação com cultivo de feijão comum seguido de milho para avaliar a eficiência agronômica e o efeito residual da adubação com PLB-N em um Argissolo Amarelo. Seis tratamentos foram testados, incluindo quatro doses de N (100, 150, 200 e 250 mg kg^{-1}) via PLB-N em aplicação única mais um controle com superfosfato triplo (TSP – aplicado de uma vez) e ureia (dividido 3 vezes) e um controle sem fertilização NP. Os poros e a superfície do BBF foram efetivamente carregados com ureia, mas não causaram sua liberação lenta, o que aumentou a salinidade do solo e reduziu temporariamente o pH do solo e afetou negativamente a produtividade do feijão comum quando comparado com a fertilização convencional (TSP + ureia). O maior efeito do PLB-N foi o residual da fertilização onde o milho apresentou uma resposta linear às doses de N aplicadas via PLB-N, mas não apresentou resposta à fertilização convencional com TSP + ureia. Portanto, o PLB-N preservou o N disponível (principalmente como NH_4^+) que foi perdido com a fertilização com N convencional. Biochar tem potencial como uma matriz de carregamento para preservar a disponibilidade de N e aumentar o efeito residual e a eficiência de uso do N pelas plantas. Os mecanismos que governam esse processo devem ser avaliados posteriormente para projetar fertilizantes de N com maior eficiência.

Palavras-chave: Liberação lenta. Especiação de fósforo. Nitrogênio. Fertilização residual. Solos tropicais.

GENERAL ABSTRACT

The association of organic biomass and inorganic sources of phosphorus (P), to obtain biochar-based fertilizers (BBFs), has been suggested to increase the efficiency of use of P in acidic tropical soils and may, additionally, increase the efficiency of use of P nitrogen (N). Although the crop's response to fertilization with BBFs has already been investigated, it is imperative to understand the forms of P in the fertilizer and the transformations of such forms of P in the soil after fertilization. Therewith, triple superphosphate (TSP) with and without MgO, phosphoric acid (H_3PO_4) with MgO were pyrolyzed with chicken litter (PLB) to produce biochar-based phosphate fertilizers (BBFs). Aiming to evaluate the agronomic efficiency of BBFs (PLB-TSP, PLB-TSP-Mg, PLB-H_3PO_4-Mg) in relation to TSP and an organomineral fertilizer (OMF), an experiment was carried out in a greenhouse with the cultivation of coffee seedlings for seven months in Clay Oxisol. The original BBFs and soil samples collected after growing were analyzed for P by conventional chemical fractionation and by X-ray absorption speciation near the edge structure (XANES). BBFs with MgO increased the efficiency of the use of P in coffee trees when compared to TSP and OMF. The results of sequential fractionation in BBFs confirmed the dominance of P associated with Ca and Mg in low solubility compounds, such as monetite and pyrophosphate identified by XANES spectroscopy. There was an increase in the labile and moderately labile fractions of P after cultivation with PLB-TSP-Mg and PLB-H_3PO_4-Mg. The results confirm that BBFs can increase the efficiency of the use of P in an Oxisol in the medium to long term and promote a greater residual effect of fertilization due to the presence of higher organic compounds. BBFs also have suitable properties to increase the efficiency of N use while providing P for the plants. In this second work carried PLB-H3PO4-Mg was loaded with 4: 5 urea (BBF: urea, w/w) aiming to generate a 15-15% NP slow-release fertilizer (PLB -N) to be used in a single application to soil. PLB-N was characterized by pH, EC, nutrient content, and P solubility and analyzed by scanning electron microscopy (SEM) and X-ray dispersive energy spectroscopy (EDX). A greenhouse experiment was carried out in carried out with cultivation of common bean followed by maize to evaluate the agronomic efficiency and the residual effect of fertilization with PLB-N in an Argissolo Amarelo (Ultisol). Six treatments were tested, including four doses of N (100, 150, 200, and 250 mg kg^{-1}) via PLB-N in single application plus a control with triple superphosphate (TSP) and urea (splitted 3 times) and a control without N-P fertilization. The pores and surface of the BBF were effectively loaded with urea but did not cause its slow-release, which increased the soil salinity and temporarily reduced the soil pH and negatively affected the yield of common bean when compared with conventional fertilization (TSP + urea). The greatest effect of PLB-N was the residual effect of fertilization where maize showed a linear response to N doses applied via PLB-N, but showed no response to the conventional TSP + urea fertilization. Therefore, PLB-N preserved available N (mainly as NH_4^+) that has been lost through conventional N fertilization. Biochar has potential as a loading matrix to preserve N availability and increase residual effect and N use efficiency by plants. The mechanisms that govern this process should be further evaluated to design increased efficiency N fertilizers.

Keywords: Slow-release. Phosphorus speciation. Nitrogen. Residual fertilization. Tropical soils.

SUMMARY

FIRST PART

GENERAL INTRODUCTION

The conversion of biomass into biochar is a blocking route to the natural carbon (C) cycle that provides environmental benefits and contributed to the development of a circular economy (HU et al., 2021). The term biochar, usually, refers to a by-product of the thermochemical conversion of organic biomass at relatively high temperatures and under oxygen-limited conditions (LEHMANN; JOSEPH, 2015). In this process, biomass undergoes decomposition, depolymerization, and condensation (WANG and WANG, 2019), which conditions the biochar to specific physical-chemical properties superior to the original feedstock. The high adsorption capacity, high specific surface area, mineral nutrients, cation exchange (CEC) and anion exchange (AEC) capacity, pH, high C content, and stable structure are some important properties that make biochar a suitable amendment for different soil types (LEHMANN and JOSEPH, 2015).

Biochar is a type of soil amendment that differs from organic compost (obtained through composting), since the organic matter in composts degrades relatively fast and becomes mineralized and requires repeated applications due to its relatively short-term persistence, while biochar can persist in the soil for a long time (TRATSCH et al., 2019). Thus, soil C sequestration, and the maintenance and/or improvement of soil quality are important issues that make the use of biochar an attractive soil amendment (LEHMANN, 2007).

The role of biochar application in increasing soil fertility can be categorized in aspects related to nutrient cycling, crop productivity, soil pH, CEC, microbial activity, water retention, and C sequestration (EL-NAGGAR et al., 2019). Therefore, the application of biochar has been increasingly recommended as a beneficial role for the retention of nitrogen (N) and phosphorus (P) in the soil. In tropical ecosystems, increasing the use efficiency of these nutrients is challenging, but an important strategy to intensify sustainable agriculture, reducing the fixation of P by the soil mineral fraction rich in Fe and Al oxides and hydroxides (NOVAIS; SMYTH, 1999) and N losses through different routes (ZHANG et al., 2015).

The biochar concentrates P and other mineral nutrients during the thermochemical conversion as opposed to C, N, O, and S (IPPOLITO et al., 2015). Thus, biochar can act as a P fertilizer and other nutrients depending on the nutrient richness in the original feedstock, although in variable quantity and availability (UCHIMIYA; HIRADATE, 2014). Additionally, biochar can affect the behavior of P in the soil, for instance the effect of biochar on soil pH influences the adsorption/desorption and the precipitation/dissolution of P minerals (BORNØ;

MÜLLER-STÖVER; LIU, 2018). There are also direct interactions between biochar and soil P, such as complexation in surface functional groups and competition of dissolved organic matter from the biochar with P ions for exchangeable sites in the soil (SCHNEIDER; HADERLEIN, 2016). Changes mediated by biochar in the soil environment can cause changes in the microbial community and alteration of the enzymatic activity (DE LUCA et al., 2015). Previously, it has been shown that the biochar application to soil could decrease the sorption capacity of P, and thus increase the P availability (CHINTALA et al., 2014; JIANG et al., 2015; MORALES et al., 2013).

Besides P, biochar can also affect significantly the N cycle (LIU et al., 2018). The application of inorganic N fertilizers in combination with the vine yard pruning biochar has been proposed to improve soil quality, crop yield, and N use efficiency (NUE), and it was indicated that adding biochar at a rate of 1% (w/w of soil) could reduce the use of inorganic N fertilizers, eventually minimizing the cost (SARFRAZ et al., 2017). Sun et al. (2017) found that the application of biochar at rates of 0.5% and 1.0% (w/w of soil) could decrease N leaching and increase its retention in saline soil. It was found that the biochar can influence the mineralization and immobilization of N (YU et al., 2021) and also affect the nitrification, denitrification, and volatilization of ammonia (DEMPSTER et al., 2012; SARFRAZ et al., 2017). The increase in the cationic and anionic exchange capacity of the soil allows the biochar to adsorb ammonium and nitrate and consequently reduce the leached N (MUKHERJEE; LAL; ZIMMERMAN, 2014). Due to the porous structure, the biochar can absorb N (GWENZI et al., 2018) and affect the N cycle influencing diversity, abundance, and microbial activities (CHEN et al., 2015).

The magnitude of the biochar effect as a soil amendment depends mainly on the biochar characteristics, which vary widely according to its source material and pyrolysis conditions (LEHMANN; JOSEPH, 2009). In a number of studies, the amount of biochar generally applied to the soil is high (> 10 t ha^{-1}), although the agronomic and economically viability of such high application rates are questionable (DING et al., 2016; ZHANG et al., 2012). In this perspective, a promising approach that has been investigated is the insertion of biochar as an additive in the process of obtaining improved efficiency fertilizers as a mixture (LUSTOSA FILHO et al., 2017; GONZÁLEZ et al., 2015; GWENZI et al., 2018) or fertilizer coating (CHEN et al., 2018; POGORZELSKI et al., 2020). This approach can be potentially attractive, sustainable and scalable, due to the cost-benefit ratio, environmentally friendly, recyclability, and possibility of producing biochar with desirable physical-chemical properties for application on an industrial scale (GONZÁLEZ et al., 2015; LEHMANN; JOSEPH, 2009).

In this perspective, some strategies have been proposed for the synthesis of biochar-based fertilizers, including co-pyrolysis (AN et al., 2020; LUSTOSA FILHO et al., 2017) or direct mixing after biomass pyrolysis (POGORZELSKI et al., 2020; SANTOS et al., 2019). Recently, a biochar-based N fertilizer obtained from mixing and granulating biochar with urea has been shown to substantially increase the N retention of the fertilizer in the soil, reducing NH_3 emissions and N leaching compared to urea alone (SAHA et al., 2018). It has also been demonstrated by scanning electron microscopy (SEM) and X-ray dispersive energy spectroscopy (EDX) that biochar is highly porous and microstructures allowing effective absorption of NO_3^-, PO_4^{3-} and K^+ (GWENZI et al., 2018).

Biochar enriched with P sources has been shown to greatly improve the biochar C stability (CARNEIRO et al., 2018; ZHAO et al., 2016), and has also shown greater efficiency in the use of plant P in highly weathered soils (CARNEIRO et al., 2021; LUSTOSA FILHO et al., 2019). In addition to increased C retention, these BBFs exhibit a slower P release behavior, due to the formation of C-O-P or C-P bonds during the co-pyrolysis process (ZHAO et al., 2016). The addition of different sources of P (TSP, MAP, H_3PO_4) with and without magnesium oxide (MgO) in co-pyrolysis of poultry litter reduced acidity from the P sources and improved performance of slow-release, due to the formation of low solubility compounds such as pyrophosphates and hydroxyapatite (LUSTOSA FILHO et al., 2017). Particularly, the incorporation of H_3PO_4 and MgO into chicken litter before pyrolysis promoted an increase in surface area and increased the cation exchange capacity in the resulting biochar (LUSTOSA FILHO et al., 2017). These characteristics favor biochar as a potential carrier of N of urea to formulate an NP fertilizer with improved efficiency for crops that can allow a reduction in the frequency of application of urea while increasing the efficiency of use of N.

Aim of this thesis and research questions

The main objectives of this work were i) to understand the forms of P both in biochar-based phosphate fertilizers and in soil treated with such fertilizers; and ii) to develop a slow-release NP fertilizer by incorporating urea in biochar-based phosphate fertilizers. In the work described in this thesis, our objective was to answer the following research questions:

Biochar-based fertilizers (BBFs) produced from poultry litter impregnated with triple superphosphate, with and without the addition of magnesium oxide (MgO) and phosphoric acid,

with the addition of MgO are efficient in providing P to a perennial crop when compared to a soluble source of P and an organomineral fertilizer?

As BBFs release P slowly into the soil compared to a soluble source, what are the solubility and chemical species of P in BBFs and BBFs-treated soil?

Does the poultry litter enriched with phosphoric acid (H_3PO_4) and MgO to produce a BBF when loaded with urea, generate a NP slow-release fertilizer that can be used in a single application dose in the soil?

REFERENCES

AN, X. et al. Copyrolysis of Biomass, Bentonite, and Nutrients as a New Strategy for the Synthesis of Improved Biochar-Based Slow-Release Fertilizers. **ACS Sustainable Chemistry and Engineering**, v. 8, n. 8, p. 3181–3190, 2020.

BORNØ, M. L.; MÜLLER-STÖVER, D. S.; LIU, F. Contrasting effects of biochar on phosphorus dynamics and bioavailability in different soil types. **Science of the Total Environment**, v. 627, 2018.

CARNEIRO, J. S. D. S. et al. Carbon Stability of Engineered Biochar-Based Phosphate Fertilizers. **ACS Sustainable Chemistry and Engineering**, v. 6, n. 11, p. 14203–14212, 2018.

CARNEIRO, J. S. DA S. et al. Long-term effect of biochar-based fertilizers application in tropical soil: Agronomic efficiency and phosphorus availability. **Science of the Total Environment**, v. 760, p. 143955, 2021.

CHEN, J. et al. Consistent increase in abundance and diversity but variable change in community composition of bacteria in topsoil of rice paddy under short term biochar treatment across three sites from South China. **Applied Soil Ecology**, v. 91, p. 68–79, 2015.

CHEN, S. et al. Preparation and characterization of slow-release fertilizer encapsulated by biochar-based waterborne copolymers. **Science of The Total Environment**, v. 615, p. 431–437, 15 fev. 2018.

CHINTALA, R. et al. Phosphorus Sorption and Availability from Biochars and Soil/Biochar Mixtures. **CLEAN - Soil, Air, Water**, v. 42, n. 5, p. 626–634, 2014.

DELUCA, T. H. et al. Biochar effects on soil nutrient transformations. In: **Biochar for Environmental Management: Science, Technology and Implementation**. p. 421–454.

DEMPSTER, D. N. et al. Decreased soil microbial biomass and nitrogen mineralisation with Eucalyptus biochar addition to a coarse textured soil. **Plant and Soil**, v. 354, n. 1–2, p. 311–324, 2012.

DING, Y. et al. Biochar to improve soil fertility. A review. **Agronomy for Sustainable Development**, v. 36, n. 2, 2016.

EL-NAGGAR, A. et al. Biochar application to low fertility soils: A review of current status, and future prospects. **Geoderma**, v. 337, n. May 2018, p. 536–554, 2019.

GONZÁLEZ, M. E. et al. Evaluation of biodegradable polymers as encapsulating agents for the development of a urea controlled-release fertilizer using biochar as support material. **Science of The Total Environment**, v. 505, p. 446–453, 1 fev. 2015.

GWENZI, W. et al. Synthesis and nutrient release patterns of a biochar-based N–P–K slow-release fertilizer. **International Journal of Environmental Science and Technology**, v. 15, n. 2, p. 405–414, 2018.

HU, Q. et al. Biochar industry to circular economy. **Science of the Total Environment**, v. 757, p. 143820, 2021.

IPPOLITO, J. A. et al. Biochar elemental composition and factors influencing nutrient retention. In: LEHMANN, J.; JOSEPH, S. (Eds.). **Biochar for Environmental Management: Science, Technology and Implementation**. London: [s.n.]. p. 139–163.

JIANG, J. et al. Mobilization of phosphate in variable-charge soils amended with biochars derived from crop straws. **Soil and Tillage Research**, v. 146, n. PB, p. 139–147, 2015.

LEHMANN, J. Bio-energy in the black. **Frontiers in Ecology and the Environment**, v. 5, n. 7, p. 381–387, 1 set. 2007.

LEHMANN, J.; JOSEPH, S. Biochar for environmental management: an introduction. In: LEHMANN, J.; JOSEPH, S. (Eds.). **Biochar for Environmental Management, Science, Technology and Implementation**. 2nd eg. ed. Routledge, New York: [s.n.]. p. 1–13, 2015.

LIU, Q. et al. How does biochar influence soil N cycle? A meta-analysis. **Plant and Soil**, v. 426, n. 1–2, p. 211–225, 2018.

LUSTOSA FILHO, J. F. et al. Co-Pyrolysis of Poultry Litter and Phosphate and Magnesium Generates Alternative Slow-Release Fertilizer Suitable for Tropical Soils. **ACS Sustainable Chemistry & Engineering**, v. 5, n. 10, p. 9043–9052, 2017b.

LUSTOSA FILHO, J. F. et al. Diffusion and phosphorus solubility of biochar-based fertilizer: Visualization, chemical assessment and availability to plants. **Soil and Tillage Research**, v. 194, n. October 2018, p. 104298, 2019.

MORALES, M. M. et al. Sorption and desorption of phosphate on biochar and biochar-soil mixtures. **Soil Use and Management**, v. 29, n. 3, p. 306–314, 1 set. 2013.

MUKHERJEE, A.; LAL, R.; ZIMMERMAN, A. R. Effects of biochar and other amendments on the physical properties and greenhouse gas emissions of an artificially degraded soil. **Science of the Total Environment**, v. 487, n. 1, p. 26–36, 2014.

NOVAIS, R. F. DE; SMYTH, T. J. Fósforo em solo e planta em condições tropicais. **Informações Agronômicas**, v. 87, p. 10–11, 1999.

POGORZELSKI, D. et al. Biochar as composite of phosphate fertilizer: Characterization and agronomic effectiveness. **Science of the Total Environment**, v. 743, p. 140604, 2020.

SAHA, B. K. et al. Nitrogen Dynamics in Soil Fertilized with Slow Release Brown Coal-Urea Fertilizers. **Scientific Reports**, v. 8, n. 1, p. 1–10, 2018.

SANTOS, S. R. et al. Biochar association with phosphate fertilizer and its influence on phosphorus use efficiency by maize. **Ciência e Agrotecnologia**, v. 43, 2019.

SARFRAZ, R. et al. Impact of integrated application of biochar and nitrogen fertilizers on maize growth and nitrogen recovery in alkaline calcareous soil. **Soil Science and Plant Nutrition**, v. 63, n. 5, p. 488–498, 2017.

SCHNEIDER, F.; HADERLEIN, S. B. Potential effects of biochar on the availability of phosphorus - mechanistic insights. **Geoderma**, v. 277, p. 83–90, 2016.

SUN, H. et al. Biochar applied with appropriate rates can reduce N leaching, keep N retention and not increase NH3 volatilization in a coastal saline soil. **Science of the Total Environment**, v. 575, p. 820–825, 2017.

TRATSCH, M. V. M. et al. Composition and mineralization of organic compost derived from composting of fruit and vegetable waste. **Revista Ceres**, v. 66, n. 4, p. 307–315, 2019.

UCHIMIYA, M.; HIRADATE, S. Pyrolysis Temperature-Dependent Changes in Dissolved Phosphorus Speciation of Plant and Manure Biochars. **Journal of Agricultural and Food Chemistry**, v. 62, n. 8, p. 1802–1809, 26 fev. 2014.

WANG, J.; WANG, S. Preparation, modification and environmental application of biochar: A review. **Journal of Cleaner Production**, v. 227, p. 1002–1022, 2019.

ZHANG, A. et al. Effect of biochar amendment on maize yield and greenhouse gas emissions from a soil organic carbon poor calcareous loamy soil from Central China Plain. **Plant and Soil**, v. 351, n. 1–2, p. 263–275, 10 fev. 2012.

ZHANG, X. et al. Managing nitrogen for sustainable development. **Nature**, v. 528, n. 7580, p. 51–59, 2015.

ZHAO, L. et al. Co-Pyrolysis of Biomass with Phosphate Fertilizers to Improve Biochar Carbon Retention, Slow Nutrient Release, and Stabilize Heavy Metals in Soil. **ACS Sustainable Chemistry & Engineering**, p. 1630−1636, 2016.

SECOND PART – ARTICLES

CHAPTER 1

Solid phase speciation and phosphorus solubility in biochar-based fertilizers: phosphorus fractionation and plant responses

Chapter prepared following the guidelines of the Geoderma (to be submitted)

Solid phase speciation and phosphorus solubility in biochar-based fertilizers: phosphorus fractionation and plant responses

Cristiane Francisca Barbosa[a], Bárbara Olinda Nardis[a], José Ferreira Lustosa Filho[b], Dehon Aparecido Correa[a], Dean Hesterberg[c] and Leônidas Carrijo Azevedo Melo[a]*.

[a]Soil Science Department, Federal University of Lavras, Lavras, Minas Gerais, Brazil;
[b]Chemistry Department, Federal University of Lavras, Lavras, Minas Gerais, Brazil
[c] Department of Crop and Soil Sciences, North Carolina State University, Box 7620, Raleigh, NC 27695, USA;
CONTACT: Leônidas Carrijo Azevedo Melo, Soil Science Department, Federal University of Lavras, Lavras, Minas Gerais, Brazil, E-mail: leonidas.melo@ufla.br

Abstract

The association of organic biomass and inorganic sources of P, either for obtaining organomineral fertilizers (OMF) or biochar-based fertilizers (BBFs), has been suggested to increase the P use efficiency in acidic tropical soils. The objective of this work was to understand the forms of P both in biochar-based phosphate fertilizers and in soil treated with such materials. Thus, triple superphosphate (TSP) with and without MgO, phosphoric acid (H_3PO_4) with MgO were pyrolyzed with poultry litter (PLB) to produce biochar-based phosphate fertilizers. A greenhouse experiment was carried out by growing coffee seedlings for seven months in a clayey Oxisol in order to evaluate the agronomic efficiency of P sources and the P speciation after cultivation. The treatments consisted of six sources of P (PLB-TSP, PLB-TSP-Mg, PLB-H_3PO_4-Mg, OMF, and TSP) and a treatment without the addition of P. The original BBFs and soil samples collected after harvest were analyzed for P by conventional chemical fractionation and by K-edge X-ray absorption near edge structure (XANES) speciation. BBFs with MgO increased the P use efficiency in coffee plants by ~10% when compared with TSP and OMF. The results of sequential fractionation in BBFs suggested the dominance of P associated with Ca and Mg in compounds such as monetite and pyrophosphate identified by XANES spectroscopy. There was an increase in the labile and moderately labile P fractions after cultivation with PLB-TSP-Mg and PLB-H_3PO_4-Mg. The results suggest that BBFs can increase the P use efficiency in an Oxisol in the medium- to long-term and promote a greater residual effect of fertilization due to the presence of higher organic compounds.

Keywords: Slow-release fertilizer, XANES, organomineral, coffee plant

1. Introduction

Phosphorus is one of the most limiting nutrient in plant development in highly weathered soils, such as the extensive tropical areas in Brazil (Roy et al., 2016). In these soils, the availability of inorganic P (Pi) is limited by rapid immobilization by the mineral fraction that is rich in kaolinite, and iron (Fe) and aluminum (Al) oxides and hydroxides (Abdala et al., 2018; Novais and Smyth, 1999). To overcome this constraint, substantial fertilization is necessary, which in addition to increasing production costs contributes to the decline of finite P resources (Withers et al., 2018). The key to optimizing the anthropogenic P cycle is to improve the plant use efficiency of P from fertilizers and recovery/reuse of P from wastes and wastewaters. This strategy reduces the consumption of resources and P loss to the environment (Withers et al., 2015).

In this perspective, the association of stabilized organic waste (post-composting) with inorganic sources of P (such as triple superphosphate-TSP) results in the production of organomineral fertilizers (OMF) (Frazão et al., 2019; Sakurada et al., 2016; Sakurada et al., 2019). OMF is supposed to have higher P use efficiency when compared with conventional soluble P sources due to the slow-release of the nutrients immobilized in the organic matter and increased P availability caused by the effect of the organic fraction (Fernandes et al., 2015; Kiehl, 2008; Malavolta et al., 2002). However, composting is a biological process that needs to go through a period of stabilization, so it is time-consuming (An et al., 2020), and contributes significantly to CO_2 emissions (Haudin et al., 2013; Wang et al., 2018). Conversely, pyrolysis can convert biomass into biochar which integrated with bioenergy can be a carbon (C) negative approach (Lehmann, 2007a) while offering advantages as a matrix to deliver nutrients more efficiently in the soil. The production of fertilizers through an improved pyrolysis process, called biochar-based fertilizers (BBFs) has emerged as an innovative proposal in which the biochar is designed to improve C sequestration capacity (Carneiro et al., 2018; Zhao et al., 2016).

The synthesis of BBFs can be made from the enrichment of biomass with inorganic sources of P in co-pyrolysis (An et al., 2020; Lustosa Filho et al., 2017; Zhao et al., 2016) or post-pyrolysis mixture (Pogorzelski et al., 2020; Santos et al., 2019). In addition, to increased C retention, these BBFs exhibit a slower P release behavior, due to the formation of C-O-P or C-P bonds during the co-pyrolysis process (Zhao et al., 2016). The addition of different P sources (TSP, MAP, H_3PO_4) with and without magnesium oxide (MgO) in co-pyrolysis of poultry litter was investigated previously by our research group. The combination of MgO with all P sources reduced the acidity from the P sources and caused a slow- and steady-release, due

to the formation of low solubility compounds such as pyrophosphates and hydroxyapatite (Lustosa Filho et al., 2017). The combination of MgO with TSP and H_3PO_4 promoted changes only in water solubility, while being similar to TSP in terms of solubility in citric acid and neutral ammonium citrate + water (NAC+H_2O) (Lustosa Filho et al., 2019). Because NAC+H_2O is used as an index of P solubility in fertilizers, which in turn generally relates to plant-available P (Borges et al., 2019), these pyrolyzed materials can be particularly beneficial for tropical soils. They can increase the P use efficiency by plants, particularly perennial crops, when applied to soils with high P adsorption capacity because of the greater residual effect of fertilization (Carneiro et al., 2021).

Determining P forms in fertilizer materials and the transformation of such forms of P in soil after fertilization are essential to understand the potential value of enhanced fertilizer and therefore allow exploring appropriate recommendations (Robinson et al., 2018). As an efficient analysis, sequential chemical fractionation based on the protocol of Hedley et al. (1982) and subsequently modified versions have been widely applied to evaluate the abundance and relative mobility of P species in soil (Abdala et al., 2018; Borges et al., 2019) and other complex matrices (Huang et al., 2018; Li et al., 2018). However, this technique provides an attempt to associate P pools with varying degrees of solubility, rather than the speciation of P *sensu stricto* (Negassa et al., 2010). On the other hand, P K-edge X-ray absorption near-edge structure (XANES) spectroscopy is an advanced and sensitive technique that is capable of characterizing the average P speciation *in situ* (Eriksson et al., 2016; Huang et al., 2018; Kruse et al., 2015).

Speciation of P in biochar has already been investigated, but most studies were interested in examining the influence of production conditions (Zwetsloot; Lehmann; Solomon, 2015) or species in the raw materials (Robinson et al., 2018; Rose et al., 2019). Although crop response to BBF fertilization has already been investigated (Lustosa Filho et al., 2019; Lustosa Filho et al., 2020), P speciation in the BBF and BBF-fertilized soil has not been deeply investigated. Therefore, we aimed i) to evaluate the efficiency of poultry litter BBFs (PLB-TSP, PLB-TSP-Mg, and PLB-H_3PO_4-Mg) on coffee growth in an Oxisol under greenhouse conditions relative to conventional P (TSP) and an organomineral (OMF) fertilizer, and ii) to determine differences in the lability and chemical speciation of P in various BBFs and in Oxisol soil reacted with BBFs and conventional inorganic (TSP) or organic fertilizers (OMF). Changes in P lability were determined using sequential chemical fractionation, where proportions of P dissolved in weak chemical extractants (H_2O and $NaHCO_3$) were considered labile P and that dissolved in stronger extractants (NaOH, HCl) or residual P were considered non-labile.

Phosphorus K-edge XANES spectroscopy was used to assess differences in P species between the BBFs and treated soil.

2. Materials and methods

2.1. Production and characterization of biochar-based fertilizers

The BBFs used in this study were previously produced and characterized, and detailed information can be found elsewhere (Lustosa Filho et al., 2017). Some selected properties of BBFs are presented in Table 1. Briefly, air-dried and milled (<1 mm) poultry litter was impregnated with triple superphosphate [TSP - Ca $(H_2PO_4)_2$]; TSP + magnesium oxide (MgO) and phosphoric acid (H_3PO_4) + MgO. Phosphate sources and MgO were mixed to achieve a P/Mg molar ratio of 1:1, and the ratio of poultry litter/phosphate source was 1:0.5 (w/w). Thereafter, the P-enriched biomass was placed in an adapted muffle furnace for pyrolysis at 500 °C at a heating rate of 10 °C min^{-1} and 2 h of holding time for complete carbonization (Zhao et al., 2014). The produced biochars were identified as follows: PLB-TSP = poultry litter biochar + TSP; PLB-TSP-Mg = poultry litter biochar + TSP + MgO; and PLB- H_3PO_4-Mg = poultry litter biochar + phosphoric acid + MgO.

The total elemental contents of the BBFs (Table 1) were determined after burning for 8 h at 500 °C in a muffle furnace followed by digestion with nitric acid (HNO_3) at 120 °C, with addition of hydrogen peroxide (H_2O_2) at the end of the digestion to oxidize organic C (Enders et al., 2012). Subsequently, the digested material was dissolved in 20 mL of 5% (v/v) HNO_3 solution and the contents of P, Ca, Mg, K, Al, Fe, Mg, Na, Si and Zn were analyzed by ICP-OES (Model Blue, Germany).

Table 1. Biochar-based phosphate fertilizers, TSP and OMF characterization

Property	PLB-TSP[b]	PLB-TSP-Mg[c]	PLB-H_3PO_4-Mg[d]	TSP[e]	OMF
pH	4.6 ± 0.01	9.1 ± 0.04	6.1 ±0.02	-	-
CEC (cmolc kg^{-1})	12.4 ± 2.2	17.5 ± 3	21.6 ± 4.0	-	-
EC (dS m^{-1})	1.8 ± 0.04	1.1 ± 0.2	0.4 ± 0.02	-	-
C (%)	24.1± 0.2	21.2 ± 0.3	19.0 ± 0.1	-	-
Total elemental content (g kg^{-1})					
P	119 ± 1	122 ± 3	164 ± 11	204	-
Ca	111 ± 4	100 ± 3	17.4 ± 1	100	-
Mg	8.6 ± 0.4	67.3 ± 0.5	93.7 ± 2	-	-
K	25.54 ± 0.7	24.72 ±0.23	16.66±0.79	-	-
Al	0.26 ±0.01	0.22±0.01	0.07±0.01	-	-
Fe	10.96±0.79	8.99±0.31	1.47±0.04	-	-
Mn	0.37±0.07	0.4±0.12	0.64±0.02	-	-
Na	1.70±0.49	1.28±0.03	0.87±0.05	-	-
Si	0.52±0.02	0.29±0.02	0.29±0.05	-	-
Zn	0.42±0.01	0.38±0.00	4.03±0.11	-	-
P solubility[a.f] (g kg^{-1})					
NAC[g]+water soluble P	55.6 ± 3	114 ± 3	147 ± 3	200	-

[a]Adapted from Lustosa Filho et al. (2019) and Lustosa Filho et al. (2017). [b]Poultry litter biochar+TSP; [c]Poultry litter biochar+TSP+MgO; [d]Poultry litter biochar+H_3PO_4+MgO; [e]Adapted from Carneiro et al. (2021); [f] Solubility measured according to Brasil (2017); [g] Neutral ammonium citrate; Mean ± standard deviation (n=3).

2.2. Coffee growth experiment

Phosphate fertilizer effects on crop growth were evaluated in a greenhouse experiment using coffee (*Coffea arabica* L., Catuaí Vermelho IAC 99) as an indicator crop. It is important to highlight that this experiment was conducted for 196 d, a short period for growth of a perennial coffee tree, but long enough for aging and stabilization of P reactions in the soil (Abdala et al., 2015a).

To reduce the influence of soil organic matter mineralization on plant nutrition, a soil sample was collected from a sub-layer (40-60 cm) of an Oxisol (Rhodic Hapludox-RH) in Lavras, Minas Gerais, Brazil (915 m altitude, 21°13′34″ S and 44°58′31″ W). The sampling site was in a forest area in the University campus. Soil samples were air-dried and passed through a 2 mm sieve for chemical and physical characterization (Silva, 2009) (Table 2). The soil was placed in plastic bags of 10 dm^3 and mixed with $CaCO_3$ + $MgCO_3$ at a Ca:Mg molar ratio of 3:1 to increase the soil base saturation to 70%, then wetted to 80% of field capacity and incubated for 30 d to ensure pH stabilization.

Table 2. Soil properties describing its natural conditions.

pH water	Ca^{2+}	Mg^{2+}	Organic C	Available P	Total P	Fe[a]	Al[a]	Clay
	$cmol_c\ kg^{-1}$		$g\ kg^{-1}$	.....	$mg\ kg^{-1}$	.....		%
4.80	0.24	0.10	11.8	0.41	1920	400	1200	64

[a]oxalate-extractable Al and Fe concentrations (Schwertmann, 1964).

After the incubation period, six-month-old, coffee seedlings were transplanted. Thereafter, the soil samples were fertilized with a nutrient solution, using soluble sources, to supply the following nutrients: N, K, S, Zn, Mn, Fe, Cu, B and Mo, applied at 100, 100, 40, 4.0, 3.66, 1.55, 1.33, 0.81 and 0.15 mg kg^{-1} of soil, respectively, following recommendations for pot experiments with plants (Novais et al., 1991). Three complementary fertilizations of N and K were performed at 55 d during coffee growth in order to reach a total added content of 300 mg kg^{-1} of soil for these nutrients.

The experiment was conducted in a completely randomized design with four replicates. Treatments consisted of five P sources (PLB-TSP, PLB-TSP-Mg, PLB-H_3PO_4-Mg, OMF, and TSP) and a control treatment without P addition was also included. Given differences on P solubility between the fertilizers, we applied the materials to an open pit made in the center of the pot for insertion of the coffee seedlings (Figure S1) at a rate corresponding to 150 mg kg^{-1} of soil based on P soluble in neutral ammonium citrate + water (NAC + H_2O) for all treatments following Borges et al. (2019). Applying at a comparable agronomic rate aimed to evaluate whether there were P speciation changes within our 196-day growth period that might affect the longer-term effectiveness of the BBF-based fertilizer relative to the OMF or inorganic fertilizer. Corresponding rates of total applied P were 154, 321, 161 and 167 mg kg^{-1} for the TSP, PLB-TSP, PLB-TSP-Mg, PLB-H_3PO_4-Mg treatments, respectively (Table 1).

A treatment with PLB only was not included due to its low level of both total and NAC-H_2O soluble P when compared with the fertilizers, which would require a much higher rate of material to be comparable to the other P sources, thereby greatly altering other soil properties like pH. Applying P doses based on soluble P contents is commonly used to compare P sources of different solubility (Chien et al., 2011; Kratz et al., 2019). After 196 d, the leaves, stem, and roots of the coffee plants were collected and washed with deionized water. The plant materials were oven-dried at 65 °C for 72 h to quantify the plant dry mass yield (PDM), and the materials were ground in a mill for chemical analyses. A representative sample of the plant material was digested in a block digestion system using concentrated nitric-perchloric acid mixture

(Malavolta et al., 1997) and P concentrations were measured by ICP-OES (Model Blue, Germany). Total P uptake by the coffee plant was calculated by multiplying P concentration by the respective dry mass yield. Approximately 200 cm^{-3} of soil was collected from the fertilized zone and homogenized and analyzed for pH (in water), available P by the resin method (Van Raij; Quaggio; Da Silva, 1986), followed by colorimetric determination (Murphy; Riley, 1962) and available sulfate (Vitti, 1989).

The relative agronomic effectiveness (RAE) was calculated by comparing each treatment to the reference fertilizer (TSP), following the equation:

$$\text{RAE } (\%) = \left(\frac{Y_{BBF}}{Y_{TSP}}\right) \text{ x } 100$$

Where Y_{BBF} is the plant dry matter yield by plants in a given BBFs fertilization treatment (g $plant^{-1}$); Y_{TSP} is the plant dry matter yield by plants in the reference treatment (TSP).

2.3. Phosphorus extractability and speciation

2.3.1. Sequential extraction in the BBFs

The modified sequential fractionation method proposed by Hedley et al. (1982) was employed to differentiate and quantify the major extractable pools of P in the BBFs (Li et al., 2018). Triplicate samples of each BBF weighing 200 mg were placed into 50 mL centrifuge tubes and then extracted at room temperature (25±3 °C) for 16 h sequentially by: 40 mL of water, 0.5 mol L^{-1} sodium bicarbonate ($NaHCO_3$, pH 8.5), 0.1 mol L^{-1} sodium hydroxide (NaOH) and 1.0 mol L^{-1} hydrochloric acid (HCl) (Qian; Jiang, 2014). After each successive extraction, the suspension was centrifuged and separated into supernatant and solid residue. The supernatant was filtered through a 0.45 μm filter, whereas the solid residue was used for the next extraction step. Concentrations of P, Ca and Mg in the supernatant were determined by ICP-OES (Model Blue, Germany). The proportion of P, Ca and Mg in the residue is the difference between the total BBF content of each element and the sum of the proportions extracted by H_2O, $NaHCO_3$, NaOH and HCl.

2.3.2. Sequential chemical fractionation in BBF-amended soils

After coffee cultivation, the soil P was sequentially fractionated using a chemical fractionation method proposed by Hedley et al. (1982), with modifications by Condron et al. (1985). The inorganic (Pi) and organic (Po) P pools were sequentially extracted from a 1.5 g soil sample in the following order: anion exchange resin (AER); 0.5 mol L^{-1} $NaHCO_3$ (pH 8.5); 0.1 mol L^{-1} NaOH; 1.0 mol L^{-1} HCl; 0.5 mol L^{-1} NaOH; and the remaining soil was dried at 50

°C and digest with sulfuric acid and hydrogen peroxide for residual P extraction. The quantification of P_i in the acid extracts was determined by the molecular absorption spectrophotometry (Murphy; Riley, 1962) and in alkaline extracts using the method proposed by Dick and Tabatabai (1977). Organic P in alkaline fractions was obtained by the difference between the total P (P_{total}), after digestion with sulfuric acid (H_2SO_4) 50% and ammonium persulfate in an autoclave set at 121 °C (USEPA, 1971), as measured by ICP-OES (Model Blue, Germany). Concentrations of Ca, Mg, Al and Fe in the extracts were also quantified by ICP-OES. Phosphorus fractions were grouped according to their lability as: labile P (P_{AER}, Pi_{Bic} and Po_{Bic}), moderately labile P ($Pi_{NaOH\text{-}0.1}$, $Po_{NaOH\text{-}0.1}$ and Pi_{HCl}) and non-labile P ($Pi_{NaOH\text{-}0.5}$, $Po_{NaOH\text{-}0.5}$ and $Pi_{Residual}$) (Cross and Schlesinger, 1995).

2.3.3. Phosphorus K-edge XANES analysis in BBFs and BBF-amended soils

Phosphorus K-edge XANES data collection for characterizing P species in BBFs particles and soil fertilized with BBF was carried out using the Soft X-ray Spectroscopy (SXS) beamline of the Brazilian Synchrotron Light Laboratory (LNLS), in Campinas-SP, Brazil. Spectra were collected from air-dried samples which had been ground and passed through a 125-mesh sieves. The particulate BBF samples and standard compounds were diluted to P concentrations of 0.15% with boron nitride powder in order to diminish self-absorption. The materials were uniformly spread on P-free double coated carbon conductive tape and mounted on a stainless-steel sample holder which was inserted into a chamber operated under vacuum conditions (~10-7 mbar). The beamline was equipped with a double crystal Si (111) monochromator, and data were collected in fluorescence mode. For energy calibration in the SXS beamline, a calcium phosphate standard was used (E0 set at 2150.7 eV) and scans were collected in the energy range of 2120 to 2220 eV. The step size was 1.0 eV from 2120 to 2145 eV; 0.2 eV from 2145 to 2180 and 0.5 eV from 2181 to 2220 eV, and time of 1.0 s per step. At least seven scans per sample were measured in order to obtain a higher signal-to-noise ratio.

The XANES data were processed using the Athena software in the Demeter suite, version 0.9.25 (Ravel; Newville, 2005). Background data were subtracted by fitting a linear model across the pre-edge region from between -30 and -10 eV relative to E0 (2151 eV), and normalized using a quadratic fit over a relative energy range from 30 to 65 eV. The spectra were fit using Linear Combination Fitting (LCF) in the energy range 2140-2180 eV (Gustafsson et al., 2020).

Linear combination fitting of P-XANES data was performed against spectra of standards that best represented the most likely P species expected for the experiment. The set of standards

included the following: calcium phosphates [octacalcium phosphate – $Ca_8H_2(PO_4)_6.5H_2O$; hydroxyapatite – $Ca_5(PO_4)_3(OH)$; brushite – $CaHPO_4.2H_2O$; monetite – $CaHPO_4$; β-tricalcium phosphate – β_$Ca_3(PO_4)_2$], magnesium phosphate ($MgHPO_4.3H_2O$), iron phosphate [goethite – α-FeOOH; hematite – α-Fe_2O_3; strengite – $FePO_4.2H_2O$; $FePO_4$ amorphous; $FePO_4$; P_ferrihydrite – P adsorption in $Fe_2^{3+}O_3.0.5H_2O$] and aluminum phosphate [variscite - $AlPO_4.2H_2O$, variscite_amorphous, $AlPO_4$; P-gibbsite – P adsorption in $Al(OH)_3$, P_caulinite – P adsorption in $Al_2Si_2O_5(OH)_4$] and organic phosphate [Phytic Na – $C_6H_{18}O_{24}P_6Na$; lecithin]. More information about these standards can be found elsewhere (Hurtarte et al., 2019).

The LCF was considered acceptable when the R factor was <0.01, varying from quaternary to tertiary LCF, excluding reference samples with negative weights until only positive ones remained, when necessary. The weights used at the end were the result of the average treatment with the shift of standards not higher than 0.5 eV and the percentage of weight attributed to each species. The sum of the weights has been normalized again so that the sum of them is equal to 1. The uncertainties presented represent only the uncertainties caused by the LCF method itself, i.e., they do not include uncertainties arising from normalization errors or energy calibration. The normalized data for each spectrum and the best fit was exported from Athena and the figures were constructed using OriginPro, 2016 (OriginLab Corporation, MA, EUA).

2.4. Statistical analysis

All greenhouse and extractable P data were checked for normal distribution by the Shapiro-Wilk test before further analyses. Subsequently, the data were subjected to analysis of variance and, when significant (p <0.05), the means were compared using the Scott-Knott test (p <0.05). Pearson correlations were performed between resin-extractable P and plant P uptake. Besides, for each fraction of the sequential fractionation of BBFs, Pearson correlations were also performed among P and Ca and Mg concentrations (p <0.05) aiming to verify the dissolution reactions of P-Ca and P-Mg compounds. All statistical analyses were performed using SISVAR software (Ferreira, 2014).

3. Results and Discussion

3.1. Coffee growth experiment

Dry matter production of coffee plants (sum of the dry weight of leaves, roots, and stems) is shown in Figure 1a. The treatments with PLB-TSP-Mg and PLB-H_3PO_4-Mg promoted higher PDM yield, with an increase of approximately 15% and 11% when compared with TSP

or OMF, respectively. No differences were observed among the treatments TSP-PLB, OMF, and TSP, with PDM yield greater than or similar to the control treatment. In part, this result can be attributed to the low P demand by coffee (Bragança et al., 2008). Nevertheless, we found statistically significant (p <0.05) differences in P uptake and RAE for some treatments (Fig. 1b, d). Furthermore, greater differences in resin-extractable soil P were observed (Fig. 1f), even though the treatments were applied at a constant NAC+H_2O extractable P rate.

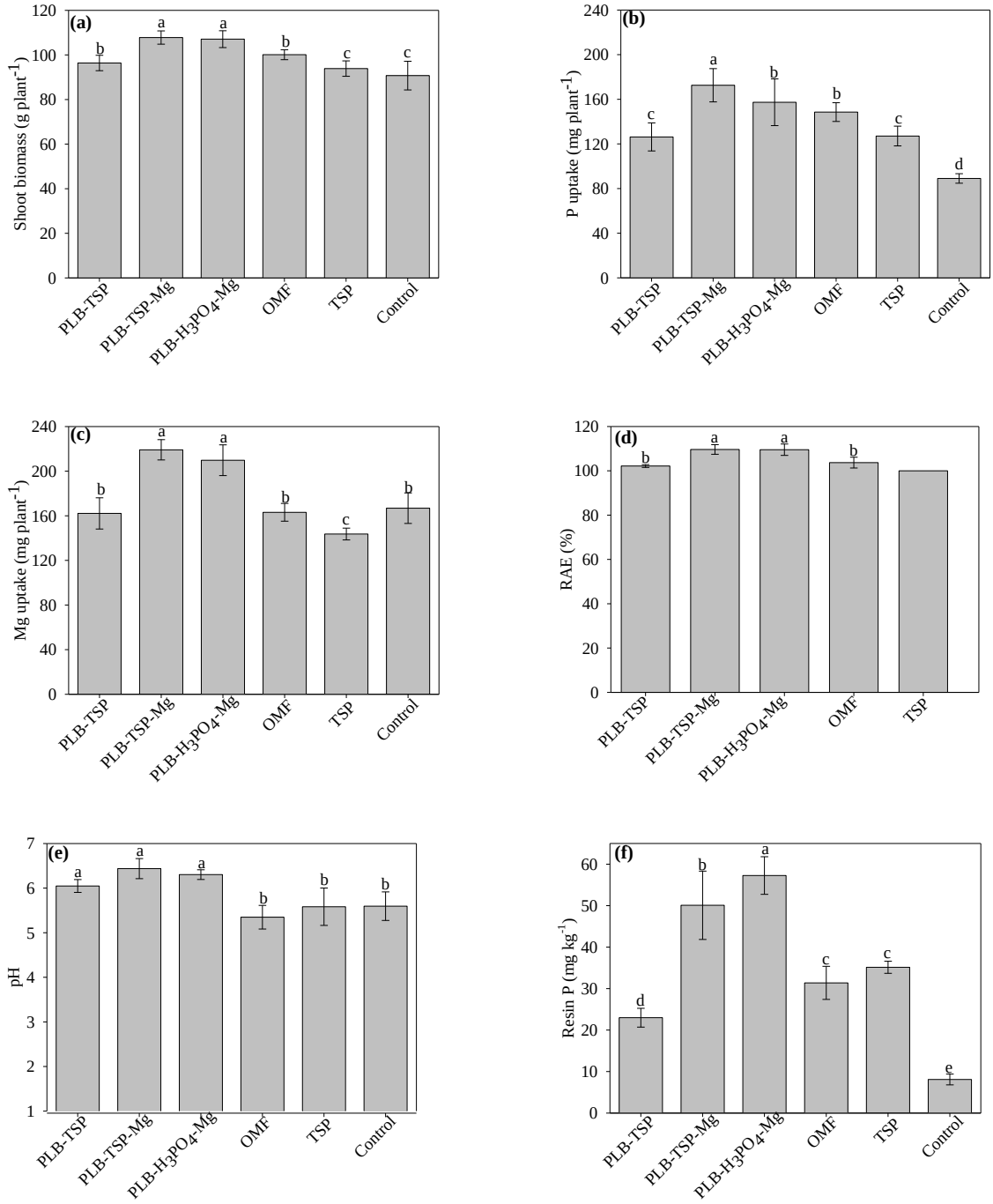

Figure 1. Shoot biomass yield (a), plant P uptake (b), plant Mg uptake (c), relative agronomic effectiveness of P (RAE) (d), soil pH (e), and soil resin P (f) after coffee cultivation. Means followed by the same letter do not differ among themselves by the Scott-Knott ($p<0.05$). Error bars represent the standard deviations of the mean (n=4).

991845923

PLB-TSP-Mg and PLB-H_3PO_4-Mg promoted greater P uptake followed by OMF (Figure 1b). The treatment with PLB-TSP showed the lowest P uptake among all P sources and did not differ significantly from the treatment with TSP (Figure 1b). The higher or lower P

uptake by the coffee plants is related to the soil P availability, which in turn is influenced by the soil pH that was higher (0.7 unit) for the Mg-containing BBFs than for the control (Figure 1d). The levels of resin-extractable P measured in the soil after cultivation followed the same trend as the other variables but with greater magnitude (Figure 1f), i.e., it was consistently higher for the treatments PLB-TSP-Mg and PLB-H_3PO_4-Mg when compared with the controls (OMF and TSP). Therefore, a strong positive correlation was observed between P uptake and levels of resin-extractable P in the soil (r = 0.91*, Figure S2a). The soil fertilized with PLB-TSP and PLB- H_3PO_4-Mg showed the highest levels of resin-extractable P, ranging from 57 to 50 mg kg^{-1}, whereas PLB-TSP had the lowest level of resin-extractable P (23 mg kg^{-1}) among the P sources studied. There was no significant difference between the soil treated with OMF and TSP, however, the latter showed equal or higher levels of resin P than the soil fertilized with PLB-TSP (Figure 1f).

The OMF used had granules of elemental sulfur (6%) that were likely oxidized (Mattiello et al., 2017) and generated enough acidity to decrease soil pH (from 6.1 to 5.3). The higher sulfate content of the soil (~14 mg kg^{-1}) in the OMF treatment supports this interpretation (Figure S2). This acidity can solubilize chemical species of Al^{3+} (Mulder; Stein, 1994), which in turn can precipitate soluble forms of P released from OMF, which might have contributed to decrease the available soil P (Figure 1f).

The relative agronomic efficiency (RAE) (Figure 1d) was ~10% higher for plants fertilized with PLB-TSP-Mg and PLB-H_3PO_4-Mg when compared with the TSP-control treatment. Moreover, PLB-TSP and OMF showed RAE similar to TSP. The differences between the RAE obtained are not fully explained by the different P water solubilities in these fertilizers, especially for the BBFs, since they generally have a lower fraction of available P as extracted by H_2O and $NaHCO_3$ (0.1 mol L^{-1}) and greater extractable P fraction with HCl (1 mol L^{-1}) (shown later). It has been implied in longer cultivation periods, the plant solubilizes less soluble P-Ca compounds by rhizosphere acidification (Freitas et al., 2013). However, treatment with PLB-TSP promoted, among the BBFs, lower PDM yield, lower P uptake, and consequently lower RAE. This demonstrates that the P use efficiency is not determined only by the solubility of the P source in NAC+H_2O.

In an analogous study with BBF and cultivation with Marandu grass (*Urochloa brizantha* cv. Marandu) (Lustosa Filho et al., 2020), it was observed that TSP showed better SDM production only in the first cultivation cycle, but BBF showed higher biomass yield after three cultivation cycles of 40 d each. The authors also observed positive correlations between P and Mg uptake only in the BBFs impregnated and MgO during the second and third crop

cycles. In our study, the highest Mg uptake was also observed by plants fertilized with PLB-TSP-Mg and PLB-H_3PO_4-Mg (Figure S2a), whereas plants in the other treatments were not significantly different ($p<0.05$) from the unfertilized control. Our results suggest that the addition of an alkaline source (MgO) to an acidic P source seems to make the greatest difference in the P use efficiency of these BBFs in the studied soil.

The association of inorganic P fertilizers with organic materials might reduce the sorption of P by soil minerals due to organic compounds blocking sorption sites (Koch et al., 2018), improving the efficiency of inorganic P fertilizers. In this study, OMF showed RAE similar to TSP, but was inferior to the BBFs enriched with MgO. In another study, an organomineral fertilizer produced from a mixture of poultry litter and TSP promoted greater P uptake, but similar yields when compared with TSP (Frazão et al., 2019). Organomineral fertilizers appears to be a promising source for improving the efficiency of P fertilization in weathered soils. BBF was shown to be as efficient or better than organomineral fertilizer (OMF), with the potential to improve the P management of mineral resources and environmental waste materials.

3.2. Phosphorus extractability and speciation

3.2.1. Sequential extraction in biochar-based fertilizers

The total content and fractions of P obtained by sequential chemical fractionation of BBFs are shown in Figure 2. The BBFs showed a relatively small fraction of the total P when extracted in H_2O and followed the order PLB-TSP (22%) > PLB-H_3PO_4-Mg (15%) > PLB-TSP-Mg (6%). The P fraction extracted with $NaHCO_3$ was higher in BBFs containing MgO, as the following order: PLB-H_3PO_4-Mg (17%) > PLB-TSP-MgO (12%) > PLB-TSP (5%). The sum of the soluble (H_2O) and exchangeable ($NaHCO_3$) P fractions are supposed to represent the readily available P for plants (Tiessen; Moir, 1993), and constituted 31% for PLB-H_3PO_4-Mg, 27% for PLB-TSP, and 18% PLB-TSP-Mg. The small fraction of readily available P relative to the total P was also verified by others (Adhikari et al., 2019; Li et al., 2018; Schneider and Haderlein, 2016), and confirms the slow-release behavior of these BBF fertilizers.

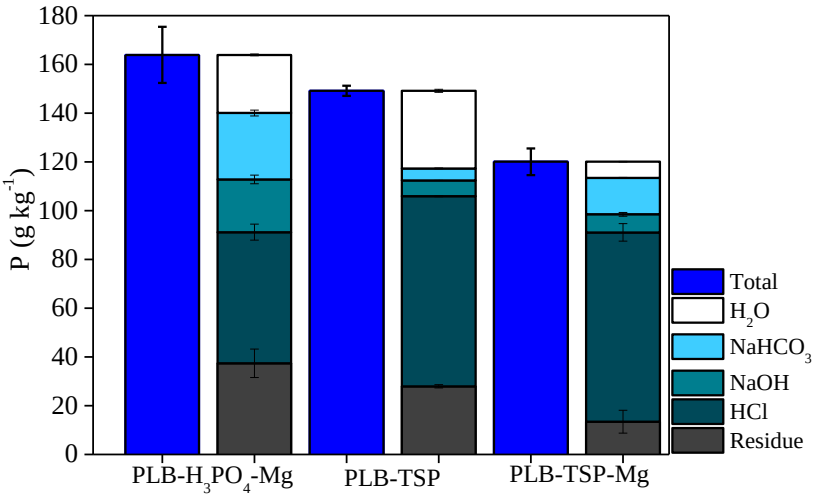

Figure 2. Total P content of biochar-based fertilizers and the P fractions obtained in sequential chemical extraction. The error bars represent the standard deviations of the mean (n = 3).

The NaOH-extractable P fraction followed the same order as for H_2O-extractable P: PLB-P-H_3PO_4-Mg (13%) > PLB-TSP-Mg (6%) > PLB-TSP (4%). The major P fraction in BBFs was extracted with HCl (Figure 2). The BBFs enriched with TSP had a considerable P fraction extracted with HCl ranging from 52% (PLB-TSP) to 64% (PLB-TSP-Mg), while for PLB-H_3PO_4-Mg this fraction represented 30%. The HCl-extractable P fraction is attributed to more stable and less soluble P compounds, which make up the structure of biochar (Huang; Tang, 2016). In addition, co-pyrolysis of PL with TSP and MgO provided greater contact of P with Ca and/or Mg, leading to the formation of insoluble Ca-P and Mg-P compounds, such as calcium pyrophosphate ($Ca_2P_2O_7$) and magnesium pyrophosphate ($Mg_2P_2O_7$) (Lustosa Filho et al., 2017).

It is assumed that the highest percentage of P extracted with HCl in BBFs is associated with the occurrence of P-Ca compounds, mainly in those BBFs enriched with TSP (Qian and Jiang, 2014). Calcium and Mg contents extracted together with P in the sequential fractionation scheme are shown in Table 3. In general, the results showed higher Ca and Mg contents in HCl extraction, reaching approximately 60% of total Ca in PLB-TSP and PLB-TSP-Mg. In BBFs enriched with MgO, the extracted Mg contents ranged from 37% to 48% for PLB-TSP-Mg and PLB-H_3PO_4-Mg, respectively.

Table 3. Contents of Ca and Mg (g kg^{-1}) detected in the P sequential fractionation extracts in PLB-TSP, PLB-TSP-Mg- and PLB-H_3PO_4-Mg and Pearson correlations between P concentration and the Ca and Mg concentrations quantified in the extracts.

Extractors	PLB-TSP		PLB-TSP-Mg		PLB-H_3PO_4-Mg	
	Ca	Mg	Ca	Mg	Ca	Mg
H_2O	6.5 ± 0.1	3.1± 0.1	0.1 ± 0.01	5.3 ± 0.2	1.25 ± 0.1	9.4 ± 0.3
$NaHCO_3$	6.7 ± 0.1	0.2± 0.01	6.5 ± 2	8.6 ± 0.2	1.25 ± 0.1	6.3 ± 0.5
NaOH	0.1 ± 0.02	-	0.02 ± 0.01	-	0.27 ± 0.1	23 ± 0.3
HCl	73.7 ± 0.3	2.2± 0.01	67.2 ± 2	33.3 ± 1.8	8.13 ± 0.2	36.3 ± 2.8
Residue	13 ± 0.4	3.1 ± 0.4	26.1 ± 0.5	20.1 ± 1.8	6.50 ± 1	40 ± 3
r^1	0.94^{ns}	0.70^{ns}	0.42^{ns}	0.98*	0.99**	0.98*

Notes: Values are mean (n = 3) ± standard error.[1] correlation coefficient, [ns] no significant, * significant with $p \leq 0.05$; ** significant with $p \leq 0.005$

These results indicate that HCl-extractable P could be linked to Ca and Mg in the BBFs. Adhikari et al. (2019) attributed the increase of the P fraction extracted with HCl in sewage sludge biochar to the increase of Ca and Mg contact in the transformation of organic matter, which would lead to the formation of insoluble P-Ca and P-Mg. The decomposition of organophosphates and/or polyphosphates results in increased association of P with metals or minerals (Huang et al., 2017). Moreover, when considering all the P fractions extracted during the sequential fractionation, PLB-P-H_3PO_4-Mg and PLB-TSP-Mg showed a strong positive correlation with Mg (r = 0.98 *), and PLB-TSP did not show correlation with Ca (r = 0.94 [ns]).

Finally, the fraction that is recalcitrant to extraction and remained in the residues was higher for PLB- H_3PO_4-Mg (23%) followed by PLB-TSP (19%) and PLB-TSP-Mg (11%). This considerable residual P content may be associated with higher fixed carbon content that causes P stabilization. The MgO and P as additives in biomass results in biochar products with a higher surface area and lower H/C ratio (Carneiro et al., 2018), indicating the formation of more aromatic structures (Gascó et al., 2018). Spectroscopic results in these BBFs suggested that a lower percentage of residual P in PLB-TSP-Mg relative to PLB-TSP is probably due to the formation of the P-O-Mg bond due to MgO addition (Carneiro et al., 2018). In the long-term, this fraction may contribute effectively in the construction of soil nutrients repository, providing fertility for growing crops (Liu et al., 2019).

It is generally considered that the P fraction extracted with H_2O and $NaHCO_3$ is plant available in the short-term, the fraction extracted with NaOH is plant available in the medium-term, but the fraction extracted with HCl can hardly be absorbed by plants directly (Qian and

Jiang, 2014). In general, BBFs presented between 18% and 31% of the readily available P, and between 50% and 64% of the total P extracted with HCl. These results, combined with the growth of coffee plants in a greenhouse, demonstrate that the sequential chemical fractions may not effectively reflect the bioavailability of P from the BBFs in the soil. Both PLB-TSP-Mg and PLB-H_3PO_4-Mg promoted greater RAE than TSP (Figure 1c), and also showed higher levels of available P in the soil after coffee cultivation. Our results also show the importance of validating the results obtained in the sequential fractionation of fertilizers with bioavailability tests. Furthermore, it should be highlighted that the P speciation by sequential extraction is operationally defined and should only be considered as a statistical inference when correlated with a designated chemical species determined by more direct spectroscopic methods (Huang and Tang, 2016; Huang et al., 2017).

3.2.2. Phosphorus Fractions in BBF-amended soils

Phosphorus fractions are presented in Figure 3 and were grouped according to their lability, and the sum of organic and inorganic P related to the total P obtained for each fraction (labile, moderately labile and non-labile) (Cross and Schlesinger, 1995). The labile P fraction was the one that least contributed to the P total in the soil (1-2%), but had its contents of Pi and Po significantly altered, to a greater or lesser magnitude, with P application (Figure 3a). The highest fraction of labile P was measured for treatment with TSP, followed by PLB-H_3PO_4-Mg and PLB-TSP-Mg. However, for the latter, Pi was the predominant form in this fraction. Among the BBFs, there was no significant difference for the treatments with PLB-H3PO4-Mg and PLB-TSP-Mg, while PLB-TSP presented the lowest fraction of labile P, which did not differ statistically from the control treatment.

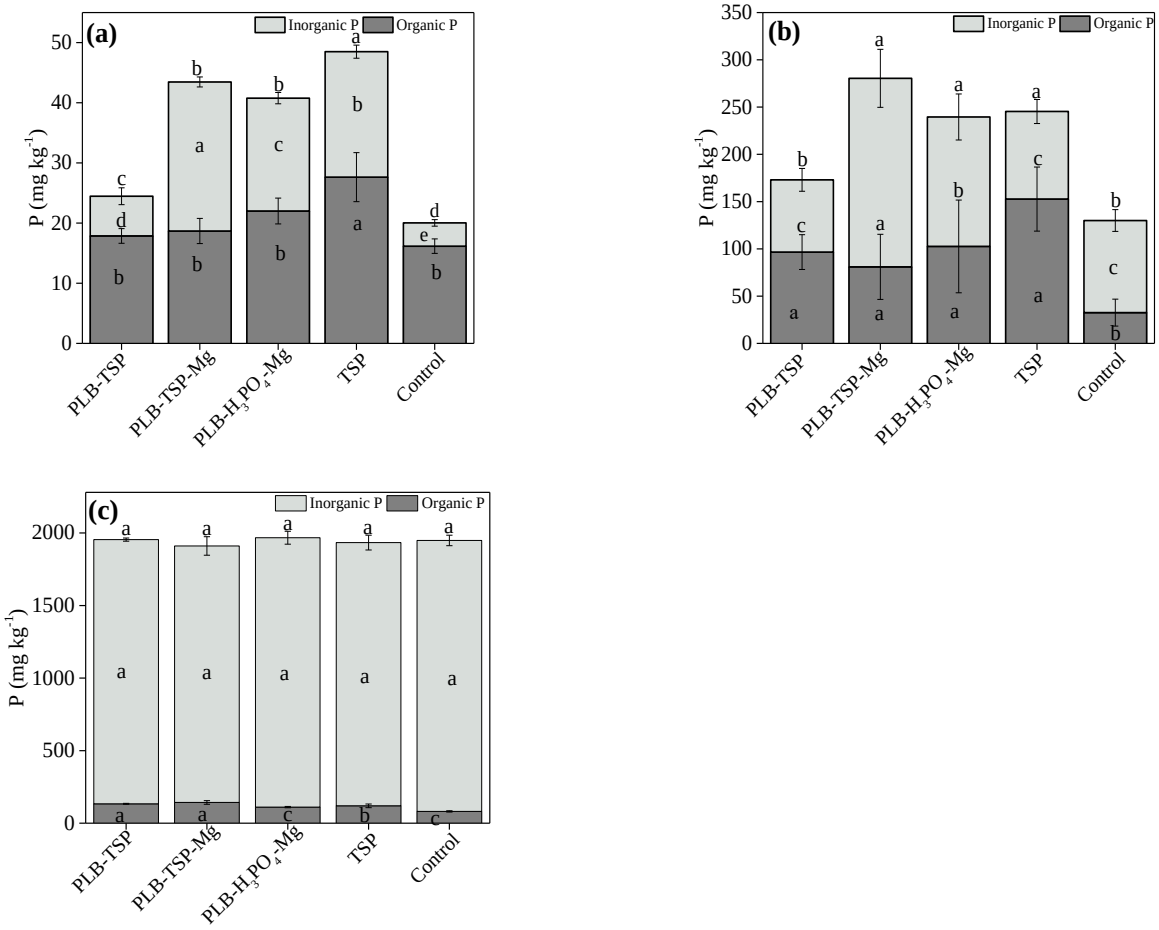

Figure 3. Labile P (P_{AER}, Pi_{Bic} and Po_{Bic}) (a); Moderately labile P ($Pi_{NaOH\text{-}0.1}$, $Po_{NaOH\text{-}0.1}$ and Pi_{HCl}) (b); Non labile P ($Pi_{NaOH\text{-}0.5}$, $Po_{NaOH\text{-}0.5}$ and $Pi_{Residual}$) (c). Means followed by the same letter do not differ among themselves by the Scott Knott test ($p < 0.05$). Error bars represent the standard deviations of the treatment mean replicates (n=4).

The lower contribution of labile P in relation to soil P stock has also been reported in other studies (Frazão et al., 2019; Lustosa Filho et al., 2020) and is typically observed in highly weathered tropical soils, due to their high capacity to immobilize the P (Teles et al., 2017). The small portion of strong P adsorbents in the soil (e.g., crystalline oxides of Fe and Al contents of 400 and 1,200 mg kg^{-1}, respectively) indicates that this was not the main factor that controlled the behavior of P by fertilizers. However, the clay fraction represents 64% of the total soil texture and is dominated by gibbsite, goethite, and hematite (Maluf et al., 2018). These minerals can adsorb P and form surface complexes of greater stability that limit the P availability to plants (Abdala et al., 2015b; Soltangheisi et al., 2018).

Treatments with PLB-TSP-Mg and PLB-H_3PO_4-Mg showed similar contents as TSP when compared with the moderately labile P fraction (Figure 3b), although Po and Pi

contributed differently. The Pi content in the soil treated with PLB-TSP-Mg was higher than the other treatments and represented 71% of the total P of this fraction. There was no difference between PLB-TSP and TSP in the contents of Po and Pi. In moderately labile P fraction, the lowest contribution was the HCl-extractable P (Table S4) and showed no difference between treatments. This indicates that during coffee growth Ca species such as monetite in the PLB-TSP-Mg and pyrophosphates in the PLB-H_3PO_4-Mg were solubilized and absorbed by the plants. This step of sequential fractionation mainly extracts more crystalline minerals and moderately soluble compounds of P bound to the surface of negatively charged oxides (Hedley et al., 1982; Soltangheisi et al., 2018).

The addition of PLB-TSP resulted in less change in the fractions of labile and moderately labile P, compared with the other P sources, with no statistical difference to the control. However, when considering Pi and Po alone, it was observed an increase in labile Pi and moderately labile Po (Figures 3a and 3b). These results are consistent with the lower biomass yield and P uptake by coffee plants. Furthermore, based on the P species obtained by XANES spectroscopy, in PLB-TSP the Po (fitted as Phytic Na) represented the predominant P species, which suggests that the reaction time in the soil may have not been sufficient to solubilize stable forms of P.

The non-labile P pool ($Pi_{NaOH-0.5}$, $Po_{NaOH-0.5}$, and $Pi_{Residual}$) was not affected by P fertilization and was dominant, representing between 86% and 92% of the total P in the soil. Our results emphasize the ability of tropical soils to strongly retain P in less soluble forms (Teles et al., 2017), due to its mineral fraction (Muljadi; Posner; Quirk, 1966). Moreover, in short-term studies like this, mild or insignificant changes are expected in the non-labile P pool. The concentrations of $Pi_{NaOH-0.5}$, were higher in treatments with BBFs compared to the other treatments (TSP and control), which can be attributed to the lower solubility of these fertilizers.

The inconsistencies found between results of sequential P fractionation and coffee growth can be partially attributed to soil sampling for analysis, since the application of P sources was located in the pit where the coffee seedling was inserted (Figure S1b). Due to practical limitations in separating fertilized soil from unfertilized soil, the sample collected may not be fully representative of the fertilized zone, but the root proliferation could be more concentrated in this zone.

The moderately labile P pool has been inferred to contributes the most to P availability for plant uptake, especially in highly weathered soils, acting as a buffer for the P extractable with $NaHCO_3$ (Almeida; Penn; Rosolem, 2018). In this study, the sum of labile and moderately labile P pools showed a good correlation with P uptake by coffee (r = 87*). Perhaps, because it

is a perennial crop that does not immediately demand high levels of available P, the sum of these pools of P might be more representative of the long-term availability of P for the plant.

3.2.3. Phosphorus K-edge XANES analysis in BBFs and BBFs-amended soils

The normalized P K-edge XANES spectra of standards (Figure 4a) showed distinctive features to identify P species and estimate their relative abundances both in BBF and soils. Phosphorus K-edge XANES spectroscopy in BBF samples, as well as in standards, revealed a prominent white line peak (Figure 4a, ii), representing the absorption edge of P (Ingall et al., 2011). In Figure 4, the post-white line shoulder (iii) and a secondary peak (iv) are normally associated with Ca or Mg minerals, the characteristic of the shoulder is associated with Ca content, and the secondary peak is associated with the degree of crystallinity (Ingall et al., 2011). A broader peak (v) is attributed to the EXAFS regions (Oxmann, 2014). The phytic acid (as Na-phytate) lacked distinct spectral characteristics, despite showing some change in the peak white line energy (ii) and peak oxygen oscillation (v), which were broader in comparison with other P species. The other P species had spectra generally without distinct signatures.

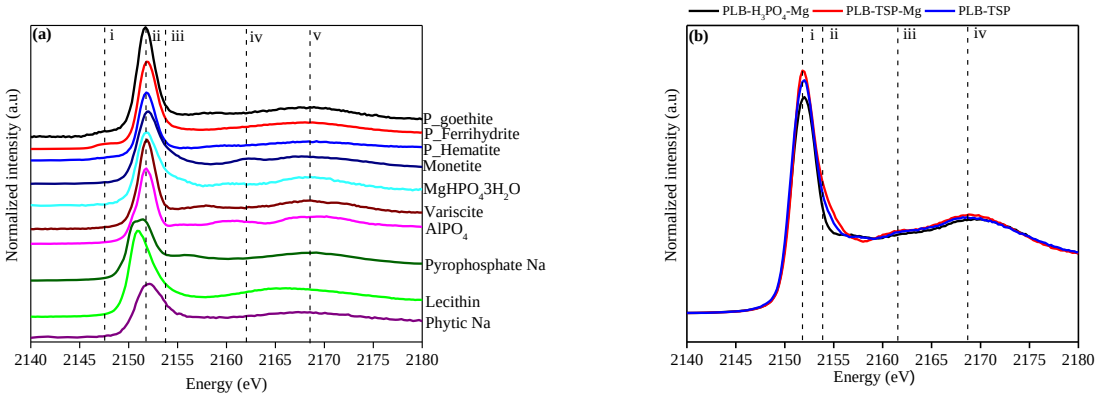

Figure 4. Phosphorus K–edge near structure (XANES) spectra of reference compounds (a) and spectra overlapping biochar-based phosphate fertilizers (b). Dashed lines indicate spectral features at i (pre-edge peak), ii (white line), ii (post-edge shoulder), iii (secondary peak), and iv (EXAFS regions).

The LCFs showed good agreement with the sample spectra (Figure S3a, b, and c) and showed some differences in the P species among the BBFs. Considering only species fitted at >5%, organic phosphate (fitted as Na-phytate) was the dominant species in fits to PLB-TSP (52.7%) (Table 4). Phytic Na constituted 31.2% and 37% of fits to PLB-TSP-Mg and PLB-H_3PO_4-Mg, respectively.

Table 4. Linear Combinations of XANES spectra from P speciation reference compounds giving the best fit to spectra for BBFs and soils in linear combination fitting. Residual (R-factor) value indicate goodness of fit. Numbers in parentheses represent uncertainties calculated by Athena.

Treatment	Standards						R-
BBFs	Variscite	P-Al[1]	Phytic Na	Monetite	P-Mg[3]	Pyro-Na[4]	factor
PLB-TSP	-	12.0±1	52.7±2	35.2±2	-	-	0.002
PLB-TSP-Mg	-	-	31.2±2	38.4±3	30.3±3	-	0.001
PLB-H_3PO_4-Mg	17.2±1	-	37.0±3	-	-	45.7±3	0.003
Soils	P-Goethite	P-Al	P-Hematite	P-Ferrihydrite	Lecithin	R-factor	
PLB-TSP	72.5±2	13.8±1	-	5.39±2	8.3±1	0.001	
PLB-TSP-Mg	-	21.3±2	35.1±2	25.5±4	18±2	0.001	
PLB-H_3PO_4-Mg	58.4±4	15.6±2	14.6±2.	11.3±2	-	0.002	
TSP	40.4±5	20.5±2	19.6±2	19.4±3	-	0.002	
Control	43.0±4	17.6±2	21.5±2	17.9±3	-	0.002	

Note [1]P-Al: non-crystalline aluminum phosphate ($AlPO_4$ x H_2O); [2]P-Mg: $Mg_3(PO_4)_2$; [4]Pyro: Pyrophosphate.

Phytic acid is commonly found in the raw material (poultry litter) (Lott et al., 2000; Toor et al., 2005), however, a lower proportion of organic phosphate was expected after pyrolysis. The appearance of organic P species seems to be linked to the co-pyrolysis of biomass with phosphate compounds that stabilize the C fraction in the biochar (Carneiro et al., 2018; Zhao et al., 2014; Zhao et al., 2017). Co-pyrolysis transformed P into forms that remained relatively resistant to subsequent pyrolysis, and part of the P captured by the aromatic rings produced during the decomposition of the organic compounds can form organic P species with greater stability. This is possibly the cause of the lower P fraction extracted in NaOH and is consistent with the P remaining in the residues after sequential chemical fractionation (Figure 2). Also, the best fit of the spectra, with this organic P compound, can be plausibly explained by the low sensitivity of this technique to identify and quantify organic P species (Kruse et al., 2015; Werner and Prietzel, 2015).

The samples of BBFs enriched with TSP indicated P species associated with Ca, fitted as monetite [$Ca(PO_3OH)$], with relative abundances of 35.2% and 38.4% for PLB-TSP and PLB-TSP-Mg, respectively. This interpretation is aligned with the appearance of a post-edge shoulder, evidenced by the superposition of the spectra of BBFs (Figure 4b, ii), which is indicative of the Ca phosphate phase (Ingall et al., 2011). The appearance of a less prominent shoulder indicates species of Ca phosphates with lower crystallinity (Bruun et al., 2017), while

better defined shoulders corresponded with Ca phosphate species with lower solubility and greater thermodynamic stability (Hesterberg et al., 1999).

The appearance of pyrophosphate, fitted as Na pyrophosphate in the PLB- H_3PO_4-Mg (45.7%), and as Mg phosphate in the PLB-TSP-Mg, likely occurred at the expense of organic P (fitted as phytic Na) (Table 4). It has been previously shown that Mg pyrophosphate ($Mg_2P_2O_7$) formed in these BBFs due to the addition of MgO was attributed to the decrease in P-O-C bonds, and partially explains the decrease in organic P (Lustosa Filho et al., 2017). Furthermore, biochar produced from plant biomass at temperatures between 350 and 650 °C showed a dominance of pyrophosphate, which was attributed to the degradation of phytates (Robinson et al., 2018; Uchimiya and Hiradate, 2014). Considering the low total Na content in the PLB-H_3PO_4-Mg (supplementary materials, Table S3), the best fit with Na pyrophosphate might be due to the limited number of pyrophosphate fitting reference compounds that was used, and we were not able to obtain a better fit by including a Mg pyrophosphate standard, for instance.

The inclusion of monetite in the fits of PLB-TSP and PLB-TSP-Mg is consistent with the results of sequential chemical extraction, and justifies the higher P fraction extracted with HCl, as discussed before. Moreover, the largest HCl-extractable P fraction in the PLB-TSP-Mg (64%) is also due to the presence of Mg phosphate (P-Mg- 30.3%), which together with monetite sum up to 69% of the total P. For these P species, the mobilization of P by crops would be stimulated by the acidification of the rhizosphere due to organic ligands and/or proton extrusion (Qin et al., 2013).

The relative abundance of P species that are potentially associated with Al, inferred from the LCF results, including variscite (17.2%) in the PLB-H_3PO_4-Mg exceeded by 21% what was stoichiometrically possible based on molar ratios of measured total Al and total P contents (Supplementary materials, Table S3). Despite this, the occurrence of variscite was consistent with the highest fraction of P extracted in NaOH (13% of total P) for PLB-H_3PO_4-Mg. Compounds with less distinct spectral characteristics cannot be precisely identified and/or quantified because LCF analysis is a modeling method that would depend on the spectral database available. Also, not all P species in complex samples can be identified by LCF analysis of the P XANES spectra because only a limited number of standards can be included without overfitting sample spectra (Huang et al., 2018).

The spectra of the standards used in LCF analysis of the P-XANES data for soils are presented in Figure 4a and the LCFs showed good agreement with sample spectra (Figure S4a, b, c, d, and e). XANES spectroscopy is adequate to distinguish P linked to different elements

(for example Al, Fe, and Ca) due to specific spectrum signatures. The P associated with Fe^{III} minerals, such as ferrihydrite, goethite and hematite, is characterized by a pre-edge peak (Figure 4a, ii) that is not visible for P linked to Al or Ca (Ingall et al., 2011). The presence of this pre-edge peak in P K-edge XANES spectra indicates phosphate adsorbed through inner-sphere surface complexes to Fe(III) in (oxy)hydroxides (Prietzel and Klysubun, 2018; Khare et al., 2007).

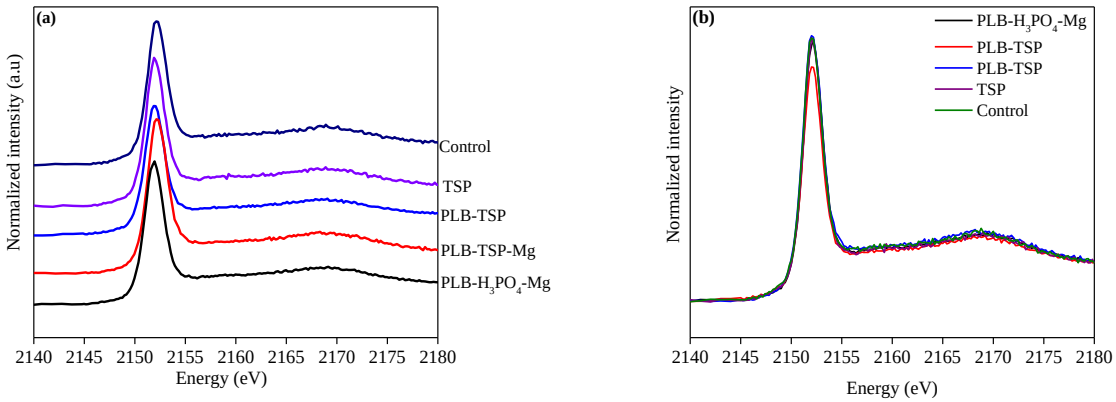

Figure 5. Phosphorus K-edge near structure (XANES) spectra of BBFs-amended soils after coffee growing (a) and spectra overlapping (b).

The spectra of fertilized and unfertilized soil showed visibly similar shapes, with a strong white-line peak near 2152 eV and with small differences in the post-edge region. However, when superimposing the spectra (Figure 5b), a greater intensity of the white line is observed in the soil corrected with PLB-H_3PO_4-Mg, PLB-TSP-Mg and TSP, indicating the solubilization of Ca and Mg bound to the phosphate and the transformation into species adsorbed in the soil. In general, LCF results indicated that P was predominantly associated with Fe-(hydr)oxides (5-72%) followed by P associated with organic compounds (0-18% fitted as lecithin) and to a lesser extent associated with Al (0- 21%).

Although fits to XANES spectra for the original P sources included Na-phytic acid, lecithin was the organic P standard that best represented organic P in soils, and it was only detected in the treatments with BBFs, except for PLB-H_3PO_4-Mg. Specifically, this organic P standard ranged from 8% to 18%, in the soil treated with PLB-TSP and PLB-TSP-Mg, respectively. Lecithin may represent the presence of more stable Po species since lecithin is

mainly composed of biomolecules that act as structural components that require a greater amount of energy for decomposition (Borges et al., 2019).

4. Conclusions

In the present study, we investigated the effect of biochar-based phosphate fertilizers on P uptake and soil P speciation for coffee cultivated for seven months, compared with a soluble phosphorus fertilizer (TSP) and a commercial organomineral fertilizer (OMF). The results showed that BBFs enriched with MgO promoted higher dry matter yield, P uptake, and greater effective use of P compared with TSP and OMF. The addition of MgO with acid P sources in BBFs is responsible in improving the efficiency of P uptake by plants. The low solubility of P in BBFs is due to the dominance of P associated with Ca and Mg in less soluble compounds, such as monetite and Na pyrophosphate as demonstrated by XANES spectroscopy. Co-pyrolysis with P compounds appeared to form organic species of greater stability that remained in the residues after sequential fractionation. BBFs were shown to increase the plant P use efficiency in a tropical Oxisol, which suggest that this class of fertilizers could promote greater residual effects of fertilization in the medium- and long-terms due to the presence of organic compounds of greater stability.

Acknowledgements

This research used resources of the Brazilian Synchrotron Light Laboratory (LNLS), an open national facility operated by the Brazilian Centre for Research in Energy and Materials (CNPEM) for the Brazilian Ministry for Science, Technology, Innovations and Communications (MCTIC). The SXS beamline staff is acknowledged for the assistance during the experiments. We are grateful to Dr. Evanise Silva Penido for the assistance with P K-edge XANES spectroscopic analysis.

Funding

This study was funded by the Brazilian funding agencies of FAPEMIG, CAPES, and CNPq. CNPq provided a PhD scholarship to C. F. Barbosa (CNPq Grant No. 149888/2016-3) and a Research Fellowship to L. C. A. Melo (Grant No. 308943/2018-0).

Conflict of interest

The authors have declared no conflict of interest.

Appendix A. Supplementary material

Supplementary information is available on the pot soil sampling (Figure S1); correlation of soil resin P and plant P uptake and sulfate levels in soil after coffee cultivation (Figure S2); best linear combination fitting results of P K-edge XANES spectra of BBFs (Figure S3) and soils (Figure S4); composition of the biochar-based fertilizers and metal/P molar ratio (Table S1); and P content in the treatments obtained by the chemical fractionation scheme (Table S2).

References

Abdala, D.B., Moore, P.A., Rodrigues, M., Herrera, W.F., Pavinato, P.S., 2018. Long-term effects of alum-treated litter, untreated litter and NH_4NO_3 application on phosphorus speciation, distribution and reactivity in soils using K-edge XANES and chemical fractionation. J. Environ. Manage. 213, 206–216. https://doi.org/10.1016/J.JENVMAN.2018.02.007.

Abdala, D.B., Northrup, P.A., Arai, Y., Sparks, D.L., 2015a. Surface loading effects on orthophosphate surface complexation at the goethite/water interface as examined by extended X-ray Absorption Fine Structure (EXAFS) spectroscopy. J. Colloid Interface Sci. 437, 297–303. https://doi.org/10.1016/j.jcis.2014.09.057.

Abdala, D.B., Northrup, P.A., Vicentin, F.C., Sparks, D.L., 2015b. Residence time and pH effects on the bonding configuration of orthophosphate surface complexes at the goethite/water interface as examined by Extended X-ray Absorption Fine Structure (EXAFS) spectroscopy. J. Colloid Interface Sci. 442, 15–21. https://doi.org/10.1016/j.jcis.2014.11.048.

Adhikari, S., Gascó, G., Méndez, A., Surapaneni, A., Jegatheesan, V., Shah, K., Paz-Ferreiro, J., 2019. Influence of pyrolysis parameters on phosphorus fractions of biosolids derived biochar. Sci. Total Environ. https://doi.org/10.1016/j.scitotenv.2019.133846.

Almeida, D.S., Penn, C.J., Rosolem, C.A., 2018. Assessment of phosphorus availability in soil cultivated with ruzigrass. Geoderma 312, 64–73. https://doi.org/10.1016/j.geoderma.2017.10.003.

An, X., Wu, Z., Yu, J., Cravotto, G., Liu, X., Li, Q., Yu, B., 2020. Copyrolysis of Biomass, Bentonite, and Nutrients as a New Strategy for the Synthesis of Improved Biochar-Based Slow-Release Fertilizers. ACS Sustain. Chem. Eng. 8, 3181–3190. https://doi.org/10.1021/acssuschemeng.9b06483.

Borges, B.M.M.N., Abdala, D.B., Souza, M.F. de, Viglio, L.M., Coelho, M.J.A., Pavinato, P.S., Franco, H.C.J., 2019. Organomineral phosphate fertilizer from sugarcane byproduct and its effects on soil phosphorus availability and sugarcane yield. Geoderma 339, 20–30. https://doi.org/10.1016/J.GEODERMA.2018.12.036.

Bragança, S.M., Martinez, H.E.P., Leite, H.G., Santos, L.P., Sediyama, C.S., Víctor, H.A. V., Lani, J.A., 2008. Accumulation of macronutrients for the Conilon coffee tree. J. Plant Nutr. 31, 103–120. https://doi.org/10.1080/01904160701741990.

Brasil, 2017. Manual de métodos analíticos oficiais para fertilizantes e corretivos. MAPA, Ministério da Agricultura Pecuária e Abastecimento/SDA, Secretaria de Defesa Agropecuária, Brasilia - DF.

Bruun, S., Harmer, S.L., Bekiaris, G., Christel, W., Zuin, L., Hu, Y., Stoumann, L., Lombi, E., 2017. Chemosphere The effect of different pyrolysis temperatures on the speciation and availability in soil of P in biochar produced from the solid fraction of manure. Chemosphere 169, 377–386. https://doi.org/10.1016/j.chemosphere.2016.11.058.

Carneiro, J.S. da S., Ribeiro, I.C.A., Nardis, B.O., Barbosa, C.F., Lustosa Filho, J.F., Melo, L.C.A., 2021. Long-term effect of biochar-based fertilizers application in tropical soil: Agronomic efficiency and phosphorus availability. Sci. Total Environ. 760, https://doi.org/10.1016/j.scitotenv.2020.143955.

Carneiro, J.S.D.S., Lustosa Filho, J.F., Nardis, B.O., Ribeiro-Soares, J., Zinn, Y.L., Melo, L.C.A., 2018. Carbon stability of engineered biochar-Based phosphate fertilizers. ACS Sustain. Chem. Eng. 6, 14203–14212. https://doi.org/10.1021/acssuschemeng.8b02841.

Chien, S.H., Prochnow, L.I., Tu, S., Snyder, C.S., 2011. Agronomic and environmental aspects of phosphate fertilizers varying in source and solubility: An update review. Nutrient Cycling. Agroecosystems. 89, 229–255. https://doi.org/10.1007/s10705-010-9390-4.

Colocho Hurtarte, L.C., Francisco, S.-F.L., Oliveira, S.W., Vergütz, L., Prietzel, J., Hesterberg, D., 2019. Optimization of data processing minimizes impact of self-absorption on phosphorus speciation results by P K-edge XANES. Soil Syst. 3.. https://doi.org/10.3390/soilsystems3030061.

Condron, L.M., GoH, K.M., Newman, R.H., 1985. Nature and distribution of soil phosphorus as revealed by a sequential extraction method followed by 31P nuclear magnetic resonance analysis. J. Soil Sci. 36, 199–207. https://doi.org/10.1111/j.1365-2389.1985.tb00324.x.

Cross, A.F., Schlesinger, W.H., 1995. A literature review and evaluation of the Hedley fractionation: Applications to the biogeochemical cycle of soil phosphorus in natural ecosystems 64, 197–214.

Dick, W.A., Tabatabai, M.A., 1977. Determination of Orthophosphate in Aqueous Solutions Containing Labile Organic and Inorganic Phosphorus Compounds1. J. Environ. Qual. 6, 82. https://doi.org/10.2134/jeq1977.00472425000600010018x.

Enders, A., Hanley, K., Whitman, T., Joseph, S., Lehmann, J., 2012. Characterization of biochars to evaluate recalcitrance and agronomic performance. Bioresour. Technol. 114, 644–653. https://doi.org/10.1016/j.biortech.2012.03.022.

Eriksson, A.K., Hesterberg, D., Klysubun, W., Gustafsson, J.P., 2016. Phosphorus dynamics in Swedish agricultural soils as influenced by fertilization and mineralogical properties: Insights gained from batch experiments and XANES spectroscopy. Sci. Total Environ. 566–567, 1410–1419. https://doi.org/10.1016/j.scitotenv.2016.05.225.

Fernandes, D.M., Grohskopf, M.A., Gomes, E.R., Ferreira, N.R., Bull, L.T., 2015. Fósforo na solução do solo em resposta à aplicação de fertilizantes fluidos mineral e organomineral. Irriga 1, 14–27. https://doi.org/DOI: 10.15809 / irriga.2015v1n1p14.

Ferreira, D.F., 2014. Sisvar: A Guide for Its Bootstrap Procedures in Multiple Comparisons Sisvar: um guia dos seus procedimentos de comparações múltiplas Bootstrap. Ciência e Agrotecnologia 38, 109–112.

Frazão, J.J., Benites, V. de M., Ribeiro, J.V.S., Pierobon, V.M., Lavres, J., 2019. Agronomic effectiveness of a granular poultry litter-derived organomineral phosphate fertilizer in tropical soils: Soil phosphorus fractionation and plant responses. Geoderma 337, 582–593. https://doi.org/10.1016/J.GEODERMA.2018.10.003.

Freitas, I.F. de, Novais, R.F., Villani, E.M. de A., Novais, S.V., 2013. Phosphorus extracted by ion exchange resins and mehlich-1 from oxisols (latosols) treated with different phosphorus rates and sources for varied soil-source contact periods. Revista. Brasileira de Ciência do Solo 37, 667–677. https://doi.org/10.1590/s0100-06832013000300013.

Gascó, G., Paz-Ferreiro, J., Álvarez, M.L., Saa, A., Méndez, A., 2018. Biochars and hydrochars prepared by pyrolysis and hydrothermal carbonisation of pig manure. Waste Manag. 79, 395–403. https://doi.org/10.1016/j.wasman.2018.08.015.

Gustafsson, J.P., Braun, S., Marius Tuyishime, J.R., Adediran, G.A., Warrinnier, R., Hesterberg, D., 2020. A probabilistic approach to phosphorus speciation of soils using p k-edge xanes spectroscopy with linear combination fitting. Soil Syst. 4, 1–17. https://doi.org/10.3390/soilsystems4020026.

Haudin, C.S., Zhang, Y., Dumény, V., Lashermes, G., Bergheaud, V., Barriuso, E., Houot, S., 2013. Fate of 14C-organic pollutant residues in composted sludge after application to soil. Chemosphere 92, 1280–1285. https://doi.org/10.1016/j.chemosphere.2013.02.041.

Hedley, M.J., Stewart, J.W.B., Chauhan, B.S., 1982. Changes in inorganic and organic soil phosphorus fractions induced by cultivation practices and by laboratory incubations 1. Solo Sci. Soc. Sou. J. 970–976.

Hesterberg, D., Zhou, W., Hutchison, K.J., Beauchemin, S., Sayers, D.E., 1999. XAFS study of adsorbed and mineral forms of phosphate. J. Synchrotron Radiat. 6, 636–638. https://doi.org/10.1107/S0909049599000370.

Huang, R., Fang, C., Lu, X., Jiang, R., Tang, Y., 2017. Transformation of phosphorus during (Hydro)thermal treatments of solid biowastes: reaction mechanisms and implications for P reclamation and recycling. Environ. Sci. Technol. 51, 10284–10298. https://doi.org/10.1021/acs.est.7b02011.

Huang, R., Fang, C., Zhang, B., Tang, Y., 2018. Transformations of phosphorus speciation during (Hydro)thermal treatments of animal manures. Environ. Sci. Technol. 52, 3016–3026. https://doi.org/10.1021/acs.est.7b05203.

Huang, R., Tang, Y., 2016. Evolution of phosphorus complexation and mineralogy during (hydro)thermal treatments of activated and anaerobically digested sludge: Insights from

sequential extraction and P K-edge XANES. Water Res. 100, 439–447. https://doi.org/10.1016/J.WATRES.2016.05.029.

Ingall, E.D., Brandes, J.A., Diaz, J.M., De Jonge, M.D., Paterson, D., McNulty, I., Elliott, W.C., Northrup, P., 2011. Phosphorus K-edge XANES spectroscopy of mineral standards. J. Synchrotron Radiat. 18, 189–197. https://doi.org/10.1107/S0909049510045322.

Khare, N., Martin, J.D., Hesterberg, D., 2007. Phosphate bonding configuration on ferrihydrite based on molecular orbital calculations and XANES fingerprinting. Geochim. Cosmochim. Acta 71, 4405–4415. https://doi.org/10.1016/j.gca.2007.07.008.

Kiehl, E. J,. Fertilizantes Organominerais, Piracicaba, 2nd ed. 2008.

Koch, M., Kruse, J., Eichler-Löbermann, B., Zimmer, D., Willbold, S., Leinweber, P., Siebers, N., 2018. Phosphorus stocks and speciation in soil profiles of a long-term fertilizer experiment: Evidence from sequential fractionation, P K-edge XANES, and 31P NMR spectroscopy. Geoderma 316, 115–126. https://doi.org/10.1016/J.GEODERMA.2017.12.003.

Kratz, S., Vogel, C., Adam, C., 2019. Agronomic performance of P recycling fertilizers and methods to predict it: a review, Nutrient Cycling in Agroecosystems. Springer Netherlands. https://doi.org/10.1007/s10705-019-10010-7.

Kruse, J., Abraham, M., Amelung, W., Baum, C., Bol, R., Kühn, O., Lewandowski, H., Niederberger, J., Oelmann, Y., Rüger, C., Santner, J., Siebers, M., Siebers, N., Spohn, M., Vestergren, J., Vogts, A., Leinweber, P., 2015. Innovative methods in soil phosphorus research: A review. J. Plant Nutr. Soil Sci. 178, 43–88. https://doi.org/10.1002/jpln.201400327.

Lehmann, J., 2007. A handful of carbon. Nature 447, 143–144. https://doi.org/10.1038/447143a.

Li, M.., Tang, Y., Lu, X.-Y., Zhang, Z., Cao, Y., 2018. Phosphorus speciation in sewage sludge and the sludge-derived biochar by a combination of experimental methods and theoretical simulation. Water Res. 140, 90–99. https://doi.org/10.1016/J.WATRES.2018.04.039.

Liu, Q., Fang, Z., Liu, Yuan, Liu, Yangyang, Xu, Y., Ruan, X., Zhang, X., Cao, W., 2019. Phosphorus speciation and bioavailability of sewage sludge derived biochar amended with CaO. Waste Manag. 87, 71–77. https://doi.org/10.1016/J.WASMAN.2019.01.045.

Lott, J.N.A., Ockenden, I., Raboy, V., Batten, G.D., 2000. Phytic acid and phosphorus in crop seeds and fruits: a global estimate. Seed Sci. Res. 10, 11–33. https://doi.org/10.1017/s0960258500000039.

Lustosa Filho, J.. F., Carneiro, J.S.D.S., Barbosa, C.F., Lima, K.P., Leite, A. do A., Melo, L. carrijo. A., Melo, A., 2020. Science of the Total Environment Aging of biochar-based fertilizers in soil : Effects on phosphorus pools and availability to Urochloa brizantha grass. Sci. Total Environ. 709, 136028. https://doi.org/10.1016/j.scitotenv.2019.136028.

Lustosa Filho, J.F., Barbosa, C.F., Carneiro, J.S. da S., Melo, L.C.A., 2019. Diffusion and phosphorus solubility of biochar-based fertilizer: Visualization, chemical assessment and

availability to plants. Soil Tillage Res. 194, 104298. https://doi.org/10.1016/j.still.2019.104298.

Lustosa Filho, J.F., Penido, E.S., Castro, P., Silva, C.A., Melo, L.C.A., 2017. Co-Pyrolysis of Poultry Litter and Phosphate and Magnesium Generates Alternative Slow-Release Fertilizer Suitable for Tropical Soils. https://doi.org/10.1021/acssuschemeng.7b01935.

Malavolta, E., Pimentel Gomes, F., Alcarde, J.C., 2002. No Title, Editora No. ed, Fertilizantes e Fertilização. São Paulo.

Malavolta, E., Vitti, G.C., Oliveira, S.A., 1997. Avaliação do estado nutricional das plantas - Princípios e aplicações. 2nd ed. Associação Brasileira para Pesquisa da Potassa e do Fósforo, Piracicaba, SP.

Maluf, H.J.G.M., Silva, C.A., Curi, N., Norton, L.D., Rosa, S.D., 2018. Adsorption and availability of phosphorus in response to humic acid rates in soils limed with $CaCO_3$ or $MgCO_3$. Ciência. e Agrotecnologia 42, 7–20. https://doi.org/10.1590/1413-70542018421014518.

Mattiello, E.M., Da Silva, R.C., Degryse, F., Baird, R., Gupta, V.V.S.R., McLaughlin, M.J., 2017. Sulfur and zinc availability from co-granulated Zn-enriched elemental sulfur fertilizers. J. Agric. Food Chem. 65, 1108–1115. https://doi.org/10.1021/acs.jafc.6b04586.

Mulder, J., Stein, A., 1994. The solubility of aluminum in acidic forest soils: Long-term changes due to acid deposition. Geochim. Cosmochim. Acta 58, 85–94. https://doi.org/10.1016/0016-7037(94)90448-0.

Muljadi, D., Posner, A.M., Quirk, J.P., 2010. The mechanism of phosphate adsorption by kaolinite, gibbsite, and pseudoboehmite. Eur. J. Soil Sci. 17, 238–247. https://doi.org/10.1111/j.1365-2389.1966.tb01467.x.

Murphy, J., Riley, J.P., 1962. A modified single solution method for the determination of phosphate in natural waters. Anal. Chim. Acta 27, 31–36. https://doi.org/10.1016/S0003-2670(00)88444-5.

Negassa, W., Kruse, J., Michalik, D., Appathurai, N., Zuin, L., Leinweber, P., 2010. Phosphorus Speciation in Agro-Industrial Byproducts: Sequential Fractionation, Solution 31 P NMR, and P K - and L 2,3 -Edge XANES Spectroscopy. Environ. Sci. Technol. 44, 2092–2097. https://doi.org/10.1021/es902963c.

Novais, R.F., Smyth, T.J., 1999. Fósforo em solo e planta em condições tropicais. Informações Agronômicas 87, 10–11.

Novais, R.F., Neves, J.C.L., Barros, N.F., 1991. Ensaio em ambiente controlado. In Métodos de pesquisa em fertilidade do solo, Embrapa-SE. ed. Brasília.

OriginPro, 2016. OriginLab Corporation, Northampton, MA, USA.

Oxmann, J.F., 2014. Technical note: An X-ray absorption method for the identification of calcium phosphate species using peak-height ratios. Biogeosciences 11, 2169–2183. https://doi.org/10.5194/bg-11-2169-2014.

Pogorzelski, D., Filho, J.F.L., Matias, P.C., Santos, W.O., Vergütz, L., Melo, L.C.A., 2020. Biochar as composite of phosphate fertilizer: Characterization and agronomic effectiveness. Sci. Total Environ. 743, 140604. https://doi.org/10.1016/j.scitotenv.2020.140604.

Prietzel, J., Klysubun, W., 2018. Phosphorus K-edge XANES spectroscopy has probably often underestimated iron oxyhydroxide-bound P in soils. J. Synchrotron Radiat. 25, 1736–1744. https://doi.org/10.1107/S1600577518013334.

Qian, L., Chen, B., 2014. Interactions of aluminum with biochars and oxidized biochars: Implications for the biochar aging process. J. Agric. Food Chem. 62, 373–380. https://doi.org/10.1021/jf404624h.

Qian, T., Jiang, H., 2014. Migration of Phosphorus in Sewage Sludge During Different Thermal Treatment Processes. https://doi.org/10.1021/sc400476j.

Qin, L., Zhang, W., Lu, J., Stack, A.G., Wang, L., 2013. Direct imaging of nanoscale dissolution of dicalcium phosphate dihydrate by an organic ligand: Concentration matters. Environ. Sci. Technol. 47, 13365–13374. https://doi.org/10.1021/es402748t

Ravel, B., Newville, M., 2005. ATHENA, ARTEMIS, HEPHAESTUS: Data analysis for X-ray absorption spectroscopy using IFEFFIT. J. Synchrotron Radiat. 12, 537–541. https://doi.org/10.1107/S0909049505012719.

Robinson, J.S., Baumann, K., Hu, Y., Hagemann, P., Kebelmann, L., Leinweber, P., 2018. Phosphorus transformations in plant-based and bio-waste materials induced by pyrolysis. Ambio 47, 73–82. https://doi.org/10.1007/s13280-017-0990-y

Rose, T.J., Schefe, C., Weng, Z., Rose, M.T., van Zwieten, L., Liu, L., Rose, A.L., 2019. Phosphorus speciation and bioavailability in diverse biochars. Plant Soil 1–12. https://doi.org/10.1007/s11104-019-04219-2.

Roy, E.D., Richards, P.D., Martinelli, L.A., Coletta, L. Della, Lins, S.R.M., Vazquez, F.F., Willig, E., Spera, S.A., VanWey, L.K., Porder, S., 2016. The phosphorus cost of agricultural intensification in the tropics. Nat. Plants 2, 16043. https://doi.org/10.1038/nplants.2016.43.

Sakurada, L.R., Muniz, A.S., Sato, F., Inoue, T.T., Neto, A.M., Batista, M.A., 2019. Chemical, Thermal, and Spectroscopic Analysis of Organomineral Fertilizer Residue Recovered from an Oxisol. https://doi.org/10.2136/sssaj2018.08.0294.
Sakurada, R., Batista, M.A., Inoue, T.T., Muniz, A.S., Pagliari, P.H., 2016. Organomineral Phosphate Fertilizers: Agronomic Effi ciency and Residual Effect on Initial Corn Development. https://doi.org/10.2134/agronj2015.0543.

Santos, S.R., Filho, J.F.L., Vergütz, L., Melo, L.C.A., 2019. Biochar association with phosphate fertilizer and its influence on phosphorus use efficiency by maize. Cienc. e Agrotecnologia 43. https://doi.org/10.1590/1413-7054201943025718.

Schneider, F., Haderlein, S.B., 2016. Potential effects of biochar on the availability of phosphorus - mechanistic insights. Geoderma 277, 83–90. https://doi.org/10.1016/j.geoderma.2016.05.007.

Schwertmann, U., 1964. Differenzierung der Eisenoxide des Bodens durch Extraktion mit Ammoniumoxalat-Lösung. Zeitschrift für Pflanzenernährung, Düngung, Bodenkd 105, 194–202. https://doi.org/10.1002/jpln.3591050303.

Silva, F.C. da, 2009. Manual de análises químicas de solos, plantas e fertilizantes, 2. ed. rev. ed. Brasília, DF: Embrapa Informação Tecnológica.

Soltangheisi, A., Rodrigues, M., Jordana, M., Coelho, A., Marcon, A., Ricardo, L., Sergio, P., 2018. Soil & Tillage Research Changes in soil phosphorus lability promoted by phosphate sources and cover crops. Soil Tillage Res. 179, 20–28. https://doi.org/10.1016/j.still.2018.01.006.

Teles, A.P.B., Rodrigues, M., Bejarano Herrera, W.F., Soltangheisi, A., Sartor, L.R., Withers, P.J.A., Pavinato, P.S., 2017. Do cover crops change the lability of phosphorus in a clayey subtropical soil under different phosphate fertilizers? Soil Use Manag. 33, 34–44. https://doi.org/10.1111/sum.12327.

Tiessen, H., Moir, J.O., 1993. No Title, in: Can. Soc. Soil Sci., L.P. (Ed.), Soil Sampling and Methods of Analysis. M.R. Carter, London, pp. 75–83.

Toor, G. S., Cade-Menun, B. J., Sims, J. T. (2005): Establishing a linkage between phosphorus forms in dairy diets, feces, and manures. J. Environ. Qual. 34, 1380–1391.

Uchimiya, M., Hiradate, S., 2014. Pyrolysis temperature-dependent changes in dissolved phosphorus speciation of plant and manure biochars. J. Agric. Food Chem. 62, 1802–1809. https://doi.org/10.1021/jf4053385.

USEPA, 1971. Methods of Chemical Analysis for Water and Wastes. Environmental Protection Agency, Cincinnati, US.

Van Raij, B., Quaggio, J.A., da Silva, N.M., 1986. Extraction of phosphorus, potassium, calcium, and magnesium from soils by an ion-exchange resin procedure. Commun. Soil Sci. Plant Anal. 17, 547–566. https://doi.org/10.1080/00103628609367733.

Vitti, G. C. O enxofre do solo. In: Bull, L. T.; Rosolem, C. A. (Ed.). Interpretação de análise química de solo e planta para fins de adubação. Botucatu: Fundação de Estudos e Pesquisas Agrícolas e Florestais, 1989. p. 129-175.

Wang, Q., Awasthi, M.K., Ren, X., Zhao, J., Li, R., Wang, Z., Wang, M., Chen, H., Zhang, Z., 2018. Combining biochar, zeolite and wood vinegar for composting of pig manure: The effect on greenhouse gas emission and nitrogen conservation. Waste Manag. 74, 221–230. https://doi.org/10.1016/j.wasman.2018.01.015.

Werner, F., Prietzel, J., 2015. Standard Protocol and Quality Assessment of Soil Phosphorus Speciation by P K-Edge XANES Spectroscopy. Environ. Sci. Technol. 49, 10521–10528. https://doi.org/10.1021/acs.est.5b03096.

Withers, P.J.A., Elser, J.J., Hilton, J., Ohtake, H., Schipper, W.J., Van Dijk, K.C., 2015. Greening the global phosphorus cycle: How green chemistry can help achieve planetary P sustainability. Green Chem. 17, 2087–2099. https://doi.org/10.1039/c4gc02445a.

Withers, P.J.A., Rodrigues, M., Soltangheisi, A., De Carvalho, T.S., Guilherme, L.R.G., Benites, V.D.M., Gatiboni, L.C., De Sousa, D.M.G., Nunes, R.D.S., Rosolem, C.A., Andreote, F.D., Oliveira, A. De, Coutinho, E.L.M., Pavinato, P.S., 2018. Transitions to sustainable management of phosphorus in Brazilian agriculture. Sci. Rep. 8. https://doi.org/10.1038/s41598-018-20887-z.

Zhao, L., Cao, X., Zheng, W., Kan, Y., 2014. Phosphorus-Assisted Biomass Thermal Conversion: Reducing Carbon Loss and Improving Biochar Stability 1–15. https://doi.org/10.1371/journal.pone.0115373

Zhao, L., Cao, X., Zheng, W., Scott, J.W., Sharma, B.K., Chen, X., 2016. Co-Pyrolysis of Biomass with Phosphate Fertilizers to Improve Biochar Carbon Retention, Slow Nutrient Release, and Stabilize Heavy Metals in Soil. ACS Sustain. Chem. Eng. 1630−1636. https://doi.org/https://doi.org/10.1021/acssuschemeng.5b01570.

Zhao, L., Zheng, W., Mašek, O., Chen, X., Gu, B., Sharma, B.K., Cao, X., 2017. Roles of Phosphoric Acid in Biochar Formation: Synchronously Improving Carbon Retention and Sorption Capacity. J. Environ. Qual. 46, 393. https://doi.org/10.2134/jeq2016.09.0344.

Zwetsloot, M.J., Lehmann, J., Solomon, D., 2015. Recycling slaughterhouse waste into fertilizer: How do pyrolysis temperature and biomass additions affect phosphorus availability and chemistry? J. Sci. Food Agric. 95, 281–288. https://doi.org/10.1002/jsfa.6716.

Supplementary Material

Solid phase speciation and phosphorus solubility in biochar-based fertilizers: phosphorus fractionation and plant responses

Figure S1. Pit in the center of the pot where the phosphorus fertilizer was applied (a); Fertilized zone where the soil was collected for chemical analysis (b); (c) Coffee plants on harvest day.

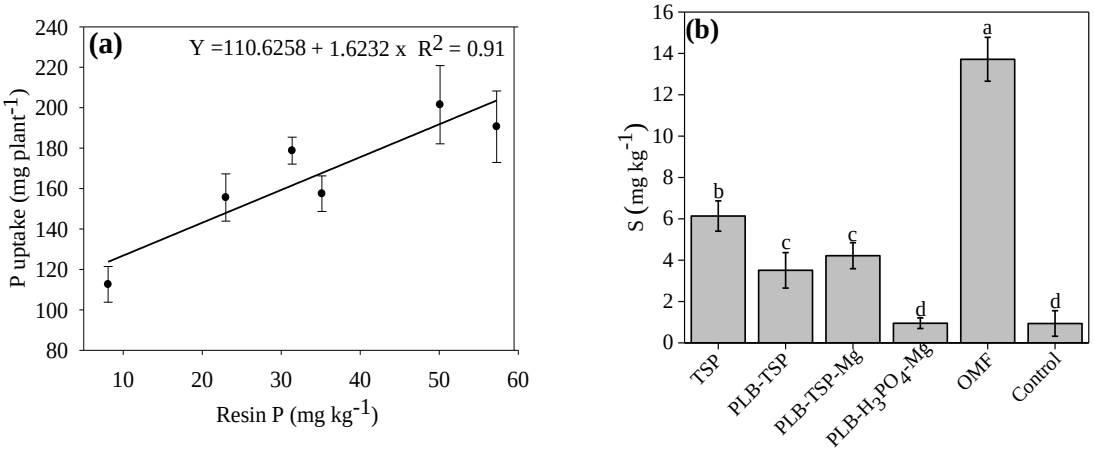

Figure S2. Scatter plot with adjusted line between P uptake by coffee and soil resin P after coffee cultivation (a), and sulfate levels in the soil after the coffee cultivation (b). Means followed by the same letter do not differ among themselves by the Scott Knott test ($p<0.05$). Error bars represent the standard deviations of the treatment mean replicates (n=4).

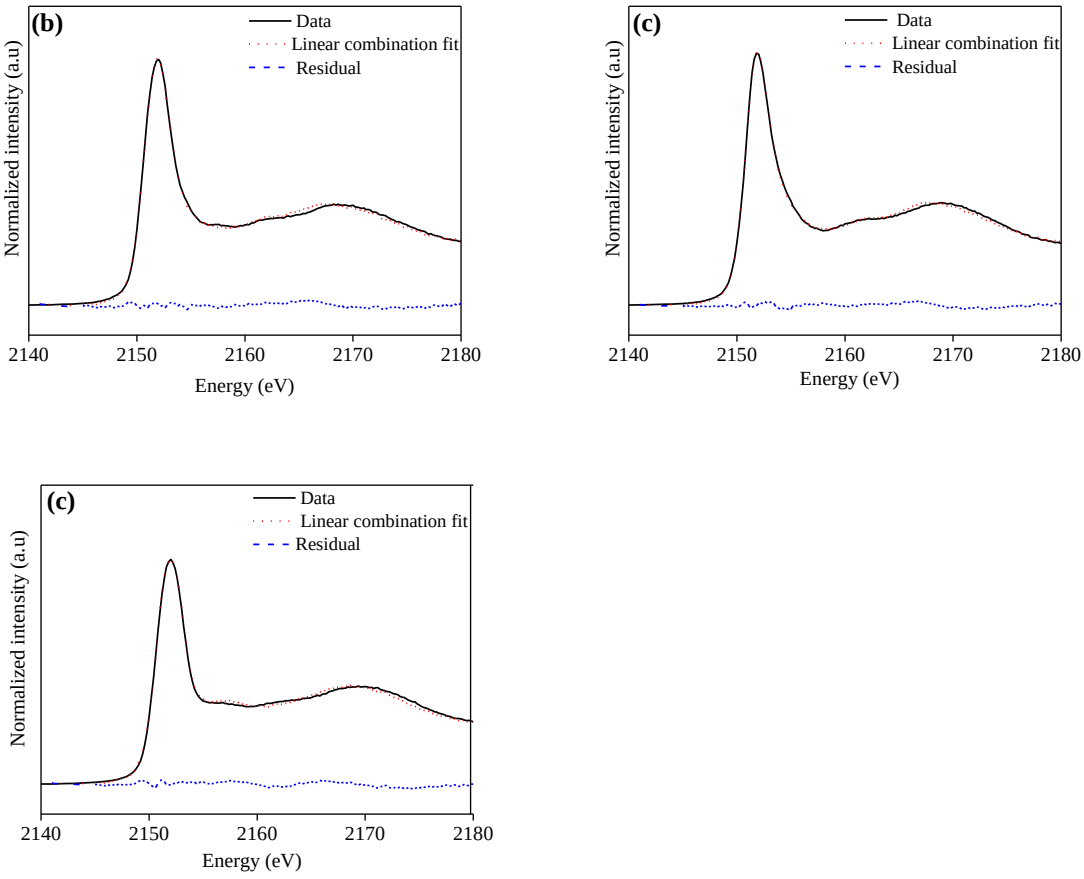

Figure S3. Best linear combination fitting results of P K-edge XANES spectra of PLB-TSP (a); PLB-TSP-Mg (b); PLB-H_3PO_4-Mg (c).

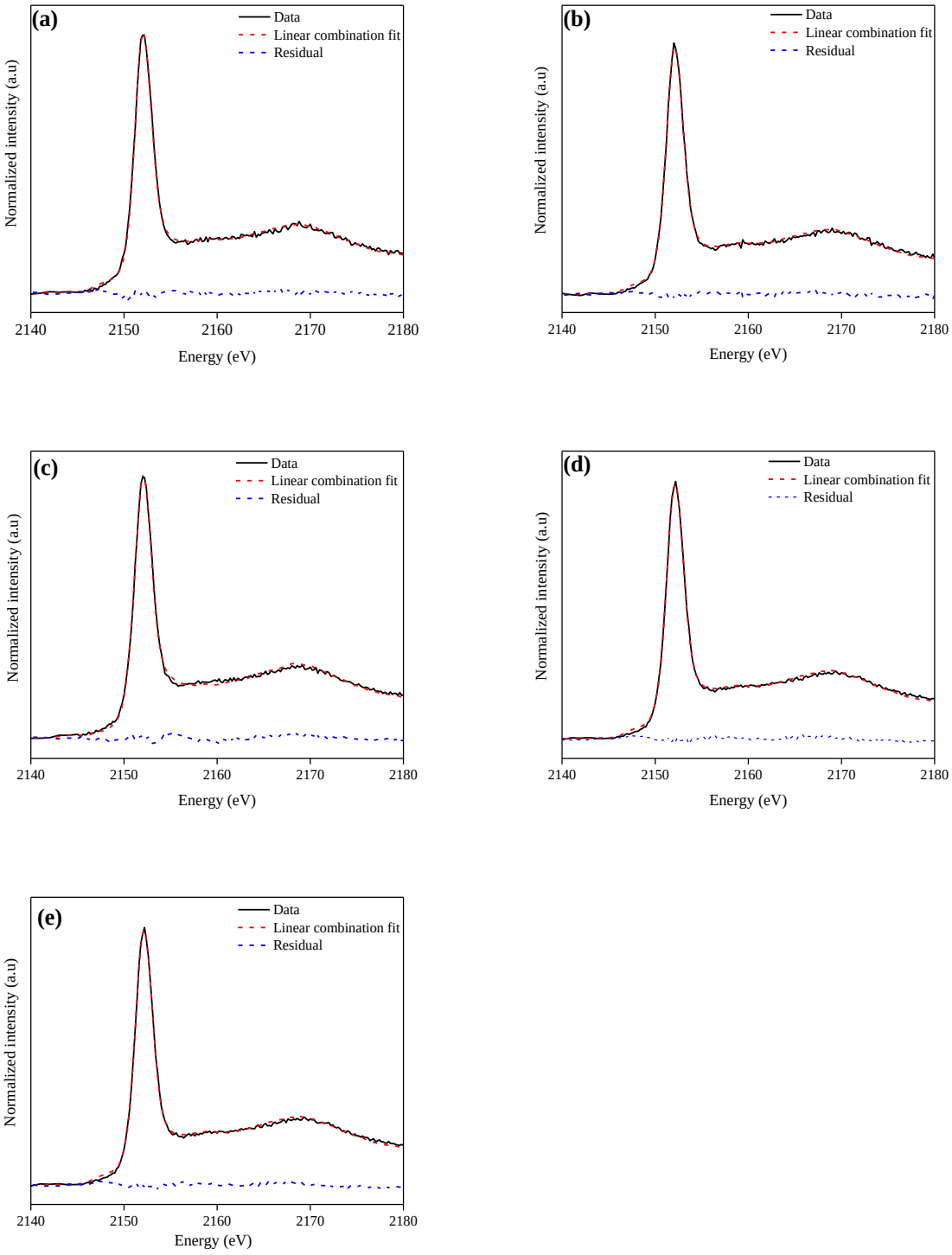

Figure S4. Best linear combination fitting results of P K-edge XANES spectra of soils after coffee growth with no applied P (control) (b) and with four sources of P: TSP (c), PLB-TSP (d), PLB-TSP-Mg (e), and PLB-H_3PO_4-Mg (f).

Table S1. Major element contents in the biochar-based fertilizers and metal/P molar ratio

Samples	P	Ca	Mg	Al	Na	Ca/P	Mg/P	Al/P	Na/P
	mol kg^{-1}					mol/mol			
PLB-TSP	4.55	3.12	0.33	0.001	0.07	0.68	0.07	0.0002	0.015
PLB-TSP-Mg	3.98	2.55	2.89	0.008	0.05	0.64	0.72	0.0020	0.012
PLB-PA-Mg	5.21	0.47	4.08	0.002	0.03	0.09	0.78	0.0004	0.005

Table S2 – Phosphorus content (mg kg^{-1}) (mean ± standard error) in inorganic and organic fractions on soil after coffee cultivation fertilized with BBFs, TSP and without fertilization (control).

	Inorganic P fractions				
Treatment	AER[a]	$NaHCO_3$	$NaOH_{0.1\ M}$[b]	HCl	$NaOH_{0.5\ M}$
PLB-TSP	2±0.2 b	5± 1 d	62± 13 c	14± 2a	17± 3a
PLB-TSP-Mg	4±0.4 a	20± 0.4 a	184± 34a	16± 2a	18±13 a
PLB-PA-Mg	5±0.8 a	14± 0.3c	122± 25b	15±1a	18±4 a
TSP	5±0.8 a	16±1 b	77± 10c	15±3 a	15± 13a
Control	0.5±0.1 b	3± 1e	86± 11 ab	12± 0.4a	11± 4b
	Organic P fractions				
	$NaHCO_3$	$NaOH_{0.1\ M}$	$NaOH_{0.5\ M}$	Residual[c]	
PLB-TSP	18± 1b	97± 18b	133± 3a	1804± 11a	
PLB-TSP-Mg	19± 2b	81± 34b	143±12 a	1750± 62b	
PLB-PA-Mg	22±2 b	103± 49b	111± 4c	1838± 45a	
TSP	28±4 a	153±33 a	120± 12b	1799± 51a	
Control	16± 1c	33± 10b	81± 4d	1856± 36a	
	Labile P	Mod-labile P[d]	Non labile P	Total P	
PLB-TSP	24±1 c	173±9b	1954±14a	2152± 16a	
PLB-TSP-Mg	44± 2a	280±33a	1910±59a	2234± 79 a	
PLB-PA-Mg	41±2b	239±34a	1967±43a	2247± 76a	
TSP	49±5a	245±45a	1934±50a	2227±75 a	
Control	20±1c	130±16b	1948±38a	2098± 30a	

Notes: Mean followed by the same letters in the columns do not differ from each other by the Scott Knott test ($p < 0.05$); [a]AER: anion exchange resin; [b]M: mol L^{-1}; [c]Difference of all inorganic and organic fractions and total P;[d] Mod-labile P: Moderately labile

CHAPTER 2

Biochar phosphate fertilizer loaded with urea preserves available nitrogen longer than conventional urea

Chapter prepared following the guidelines of the Archives of Agronomy and Soil Science (to be submitted)

Biochar phosphate fertilizer loaded with urea preserves available nitrogen longer than conventional urea

Cristiane Francisca Barbosa[a], Dehon Aparecido Correa[a], Jefferson Santana da Silva Carneiro[a] and Leônidas Carrijo Azevedo Melo[a]

[a]Soil Science Department, Federal University of Lavras, 37200-900 Lavras, Minas Gerais, Brazil

Abstract

Biochar, a carbon-rich material obtained by pyrolysis of organic wastes, is an attractive matrix to load nutrients and produce enhanced efficiency fertilizers. In this study, poultry litter (PL) was enriched with phosphoric acid (H_3PO_4) and MgO to produce a biochar-based fertilizer (PLB), which was loaded with urea in a 4:5 ratio (PLB: urea, w/w) aiming to generate a 15-15% N-P slow-release fertilizer (PLB-N) to be used in a single application to soil. PLB-N was characterized by pH, EC, nutrient contents and P solubility and analyzed by Fourier transform infrared (FTIR), and scanning electron microscopy (SEM) associated with energy-dispersive X-ray spectroscopy (EDX) analysis. A greenhouse experiment was carried out with cultivation of common bean followed by maize to evaluate the agronomic efficiency and the residual effect of fertilization with PLB-N in an Argissolo Amarelo (Ultisol). Six treatments were tested, including four doses of N (100, 150, 200, and 250 mg kg^{-1}) via PLB-N in single application, a control with triple superphosphate (TSP – applied once) and urea (splitted 3 times) and a control without N-P fertilization. The pores and surface of the BBF were effectively loaded with urea but did not reduce its hydrolysis rate, which increased the soil salinity and temporarily reduced the soil pH, which negatively affected the yield of common bean when compared with conventional fertilization (TSP + urea). The greatest effect of PLB-N was the residual effect of fertilization where maize showed a linear response to N doses applied via PLB-N, but showed no response to the conventional TSP + urea fertilization. Therefore, PLB-N preserved available N (mainly as NH_4^+) that has been lost through conventional N fertilization. Biochar has potential as a loading matrix to preserve N availability and increase residual effect and N use efficiency by plants. The mechanisms that govern this process should be further evaluated to design increased efficiency N fertilizers.

Keywords: Slow-release, nitrogen, soil fertility, residual fertilization, tropical soils.

Introduction

Soil fertilization is a key factor for agricultural production, either in quality and quantity. Among the nutrients, nitrogen (N) is the most widely applied to maintain soil fertility and crop growth (Wen et al. 2017). Synthetic N fertilizer has been a critical component of agriculture, currently accounting for more than 50% of world food production (Erisman et al. 2008; Zhang et al. 2015), while its deficiency results in reduced productivity and losses in production systems (Lu and Tian 2017). Conversely, N overload leads to environmental pollution and threatens agricultural productivity, food security, and human health (Zhang et al. 2015).

More than 50% of synthetic N fertilizers added to soil is lost through leaching, denitrification or volatilization (Fageria and Baligar, 2005; Zhang et al. 2015), which negatively impacts the environment. The main factors responsible for these losses include the low N retention capacity in soil, mineralization, and the spatial and temporal incompatibility between the application of fertilizers and crop N demand (Bowles et al. 2018). These losses collectively cause low N use efficiency (Bindraban et al. 2020) and contribute to low economic efficiency by increasing agricultural production costs (Saha et al. 2018). Nitrogen losses can be minimized through some strategies that include the use of enhanced efficiency fertilizers (EEFs) (Chen et al. 2017).

Various types of EEFs have emerged, including the use of biochar as a support material for nutrient loading (González et al. 2015; Gwenzi et al. 2018; Wen et al. 2017). Biochar is a carbonaceous material obtained from pyrolysis of wood biomass, vegetable or animal waste at moderately to high temperatures (Lehmann and Joseph 2015). The stable carbon (C) fraction, surface area, porosity and functional groups are favorable characteristics of biochar to retain nutrients (Li et al. 2018; Lehmann and Joseph, 2015; Nardis et al. 2020), which makes it attractive as a fertilizer enhancer.

Biochar-based N fertilizers are promising for sustainable agricultural development, mitigating N losses and increasing soil C stocks (Puga et al. 2019). In a recent study, Saha et al. (2018) showed that mixing and granulating biochar with urea substantially increased N retention from the fertilizer in the soil, reducing NH_3 emissions and N leaching compared with urea alone. It has been shown through scanning electron microscopy (SEM) and energy-dispersive X-ray spectroscopy (EDX) that the coarse and porous microstructure of biochar can effectively absorb NO_3^-, PO_4^{3-} and K^+ and form biochar impregnated with these nutrients (Gwenzi et al. 2018). Puga et al. (2019) used acidified biochar (pH ~3) as additive for coating urea granules and observed significantly reduction in NH_3 volatilization. Shi et al. (2020)

developed a biochar-mineral urea composite and observed a reduced release rate of N and higher shoot and roots of maize when compared with conventional urea, which was attributed to the N retention on biochar/mineral surfaces and by C bonds from urea to the biochar.

Biochar enriched with P sources were shown to improve greatly the C stability (Carneiro et al. 2018; Zhao et al. 2016), and also showed increased plant P use efficiency in highly weathered soils (Lustosa Filho et al. 2019; Carneiro et al. 2021). The addition of MgO with acid P sources reduced acidity and reduced P water solubility, but show similar solubility in citric acid and neutral ammonium citrate + water (NAC + H_2O) to TSP (Lustosa filho et al. 2019), which favors its use in P fixing tropical soils (Carneiro et al. 2021).

The combination poultry litter with H_3PO_4 and MgO prior to pyrolysis increase the specific surface area (Carneiro et al. 2018) and increase cation exchange capacity in the resulting biochar (Lustosa Filho et al. 2017). These characteristics favors biochar as a potential carrier of urea N to formulate enhanced efficiency a N-P fertilizer for crops that might allow reduction in the frequency of urea application while increase N use efficiency. In this study, we hypothesized that biochar enriched with phosphate and loaded with urea will provide greater N use efficiency by plants from a single application with higher residual effect of N and P fertilization for the subsequent crop.

Materials and methods

Production and characterization of biochar-based fertilizers

The biochar used in this study was produced from poultry litter (PLB) (Table 1) collected from a farm near Lavras, Minas Gerais, Brazil (44°58′31″ W). Briefly, air-dried and milled (<1 mm) poultry litter was impregnated with phosphoric acid (H_3PO_4) + MgO. Phosphorus and Mg were mixed to a molar ratio of 1:1 and the feedstock: phosphate at a ratio of 1:0.5 (w/w). Thereafter, the P-enriched biomass was placed in a hermetically sealed metal reactor (model SPPT-V60) for pyrolysis at 500 °C at a heating rate of 10 ° C min^{-1} and 2 h of holding time for complete carbonization. After the pyrolysis process, the biochar-based fertilizer (BBF) remained in the reactor until it reached room temperature (~16 h). The produced biochar was identified as PLB = poultry litter biochar + phosphoric acid + MgO.

Electrical conductivity (EC) and pH were obtained, in triplicate, using 1.0 g of biochar in 20 mL of deionized water and after 1.5 h of shaking (Rajkovich et al. 2012). Elemental composition of C was measured, in duplicate, using an elemental analyzer (model Vario TOC cube, Elementary, Germany). The total nutrient content was determined after burning for 8 h at

500 °C in a muffle furnace followed by digestion with nitric acid (HNO_3) at 120 °C, with addition of hydrogen peroxide (H_2O_2) at the end of the digestion to oxidize organic C (Enders et al., 2012). Subsequently, the digested material was dissolved in 20 mL of 5% (v/v) HNO_3 solution. Water-soluble P contents, citric acid-soluble P and neutral ammonium citrate NAC+H_2O-soluble P were determined according to official P fertilizer methods as described in Brasil (2014). The content of P and Mg, and the P fractions in the fertilizer were quantified by ICP-OES (Model Blue, Germany).

Procedure of production of biochar-based phosphate fertilizer enriched with urea

The process of impregnating PLB with N was carried out as described by Gwenzi et al. (2018). Briefly, a solution containing N, from the dissolution of urea [$CO(NH_2)_2$, 45% N] in deionized water was prepared and added to PLB at 4:5 ratio (PLB: Urea). The mixture was stirred for 2 h on a bench-top shaker at 100 rpm and then dried at room temperature. The biochar-based phosphate fertilizer enriched with N was thereafter named PLB-N. Urea was selected as a source of N because it is the most used N fertilizer due to its high N content and lower cost when compared with other N sources (Trenkel 2013).

Scanning electron microscopy (SEM), energy-dispersive X-ray spectroscopy (EDX) and Fourier transform infrared (FTIR) spectroscopic characterization analysis

The microscopic and morphological characteristics were characterized by scanning electron microscopy (SEM) (LEO EVO 40 XVP - Carl Zeiss) equipped with an energy-dispersive X-ray spectroscopy (Brunker - Quantax EDX). The samples were dried and coated with carbon prior to measurements using the SEM detector for 100x, 500x and 1000x magnifications. The Fourier transform infrared (FTIR) spectroscopic characterization of the urea and PLB, before and after urea impregnation, was performed with a Varian 600-IR spectrometer with a spectral range 4000-400 cm^{-1}. Oven-dried samples were ground to a powder, and the FTIR spectra with a resolution of 4 cm^{-1} were collected over an average of 32 scans.

Greenhouse pot experiment

Soil samples and preparation

Samples of a Latossolo Amarelo (Ultisol) were collected from the top layer (0-30 cm) in a cultivated area, after liming, in a farm at Country Pimenta in Lavras, Minas Gerais, MG, Brazil (21° 16’ 14” S and 45° 04’ 07” W). The soil sample was collected 90 days after the correction of soil acidity with dolomitic limestone, aiming to raise the base saturation to 70%.

After collection, the soil sample was air-dried and passed through a 2-mm mesh sieve for chemical and textural analysis (Silva, 2009), whose properties before and after liming are presented in Table 1.

Table 1. Selected properties of the soil before and after liming and prior to cultivation.

Properties	After liming
pH water	6.3
Ca^{2+} ($cmol_c\ kg^{-1}$)	2.96
Al^{3+} ($cmol_c\ kg^{-1}$)	0.06
H+Al ($cmol_c\ kg^{-1}$)	2.35
Mg^{2+} ($cmol_c\ kg^{-1}$)	1.1
Resin P ($mg\ kg^{-1}$)	10.8
P-rem ($mg\ L^{-1}$)	28.2
K ($mg\ kg^{-1}$)	161
SB ($cmol_c\ kg^{-1}$)	4.45
t ($cmol_c\ kg^{-1}$)	4.51
T ($cmol_c\ kg^{-1}$)	6.80
m (%)	1.33
V (%)	65
Organic matter (%)	2.21
Clay (%)	47
Silt (%)	11
Sand (%)	42

P-rem: remaining phosphorus after shaking with initial P of 60 $mg\ L^{-1}$; H+Al: potential acidity; t: effective cation-exchange capacity (SB+Al); T: cation-exchange capacity at pH 7.0 SB+ (H+Al); m: aluminum saturation (Al^{3+}/t); V: base saturation (SB/T); SB: sum of bases Ca, Mg and K.

Finally, 3 kg of air-dried and homogenized soil samples were placed in pots and fertilized with a nutrient solution with soluble sources to provide the following nutrient and respective contents (in mg kg): K, S, Zn, Mn, Fe, Cu, B, and Mo, applied at 100, 40, 4.0, 3.66, 1.55, 1.33, 0.81 and 0.15 $mg\ kg^{-1}$, following recommendations for pot experiments with plants (Novais et al. 1991).

Experimental design and plant growth

The experiment was carried out in a completely randomized design with four replications. Six treatments were studied including four doses of N (100, 150, 200 and 250 mg kg^{-1}) via PLB-N that supplied, respectively, 60, 90, 120 and 150 mg kg^{-1} of P soluble in NAC+H_2O; a control with triple superphosphate (200 mg kg^{-1} of P soluble in NAC+H_2O) + urea (200 mg kg^{-1} of N); and a control without P and N fertilization. The doses of N and P via PLB-N fertilizer were fully applied in powder form and incorporated into the entire volume of soil before sowing. In the conventional fertilizer control, the dose of urea was applied as a solution and splitted into three fertilizations, being 50 mg kg^{-1} at sowing and 75 mg kg^{-1} at 15 and 30 days after sowing.

Two successive cultivations were carried out as follows: in the first planting, five bean seeds (*Phaseolus vulgaris* L, cv BRSMG UAI) were sown in each pot and thinned seven days after emergence, keeping two plants per pot that were grown for 45 days. In the second cultivation, five maize seeds (*Zea mays*) were sown in each pot and thinned seven days after emergence, leaving one plant per pot, which was grown for 50 days. All nutrients were supplied as described only before the first cultivation.

Plant and soil analysis

After each growth cycle, beans followed by maize, the plants were cut at 1 cm above the soil surface and rinsed with deionized water. The plant materials were oven-dried at 65 ° C until weight stabilization (~ 72 h), and the shoot dry mass (SDM) was recorded before griding in a mill. The N content was determined by Kjeldahl method (Bremner and Mulvaney, 1982). A sample (0.5 g) of plant material was digested in a block digestion system using a concentrated nitric-perchloric acid mixture (Malavolta et al. 1997) and P was measured in the extract by ICP-OES (Model Blue, Germany). Nitrogen and P uptake were estimated by multiplying N or P concentration by the respective shoot dry mass yield. The relative agronomic effectiveness (RAE) was calculated by comparing each treatment to the reference fertilizer (Urea) added at the same fertilization dose, following equation:

$$\text{RAE } (\%) = \left(\frac{N_{PLB\text{-}N}}{N_{urea}}\right) \text{ x } 100$$

Where $N_{PLB\text{-}N}$ is the dry matter production by plants in a given PLB-N fertilization treatment (g $plant^{-1}$); N_{urea} is the dry matter production by plants in the reference treatment (urea).

After each cultivation, 30 g of soil was collected from each pot to determine the pH in water, electrical conductivity (EC), available resin P (Raij et al., 1986), with P determined molecular absorption spectrophotometry (Murphy and Riley 1962), and the inorganic forms of N, ammonium (NH_4^+) and nitrate (NO_3^-), which were determined by distillation (Cantarella and Trivelin, 2001).

Statistical analysis

All greenhouse data were checked for normal distribution by the Shapiro-Wilk test before further analysis. Subsequently, the data were subjected to analysis of variance and, when significant (p <0.05), the means were compared using the Scott Knott test (p <0.05) and the N doses were adjusted to linear regressions models. All statistical analyses were performed using SISVAR software (Ferreira, 2014).

Results and discussion

Properties of the biochar-based fertilizers

The selected properties of PL and PLB are shown in Table 1. The pyrolysis of PL enriched with H_3PO_4+MgO caused a decrease in the pH of the PLB (from 8.3 in PL to 6.1 in PLB). Normally, pristine pure PL biochar tends to be strongly alkaline (pH ~ 11), but with the impregnation of H_3PO_4 in combination with MgO eliminated the acidity of the P source (Lustosa Filho et al. 2017; Carneiro et al. 2018). There was a considerable increase in the total P content with the impregnation of H_3PO_4 and MgO (Table 1), reaching values as high as in conventional P fertilizers.

Table 1. Selected properties of poultry litter (PL) and biochar-based phosphate fertilizer (PLB).

Property	PL	PLB
pH	8.2 ± 0.02[a]	6.1 ± 0.1
EC (dS m^{-1})	4.03 ± 0.04[b]	0.46 ± 0.07
Carbon (%)	36.1 ± 0.2[a]	24. 9 ± 1.0
Total content (g kg^{-1})		
P	15.6 ± 0.4[a]	164 ± 2
Mg	5.40 ±0.20[a]	96.1 ± 3.1
P solubility (g kg^{-1})		
Water soluble	-	6.13 ± 0.12
Citric acid soluble	-	72.8 ± 3.4
NAC[c] + water-soluble	-	142 ± 6

[a] Carneiro et al. 2018; [b] Leite et al. 2020. [c]Neutral ammonium citrate; Values are mean ± standard deviation (n=3).

The P solubility in citric acid and NAC + H_2O in PLB corresponded to 44.4% and 86.6%, respectively, of the total P, while the water-soluble P of PLB was very low (3.7%) (Table 1). During pyrolysis several reactions between P and Ca and Mg take place forming insoluble P compounds such as calcium pyrophosphates ($Ca_2P_2O_7$) and magnesium pyrophosphates ($Mg_2P_2O_7$) (Lustosa Filho et al. 2017). Besides, reactions between C and P might also occur during pyrolysis and form stable P forms such as C-O-P or C-P bonds (Zhao et al. 2016).

Reducing the solubility of P in water without decreasing the solubility in NAC + H_2O might be a particularly beneficial strategy for P-fixing soils (Lustosa Filho et al. 2019), since the availability of inorganic P is limited by rapid immobilization by the mineral fraction rich in iron (Fe) and aluminum (Al) oxides (Abdala et al. 2018; Novais and Smyth, 1999).

Scanning electron microscopy (SEM) and energy-dispersive X-ray spectroscopy (EDX) analysis

The structure of the PLB surface before and after urea impregnation was characterized by scanning electron microscopy (SEM), and the results are shown in Figure 1. The PLB surface was rough and porous (Figure 1a, b, and c), while after impregnation with urea, the surface of the particles was coated with urea and the pores filled (Figure d, e, and f). The urea solubilized

in water managed to infiltrate the pores of the biochar surface and even formed a plane on the surface, thus forming a coating layer.

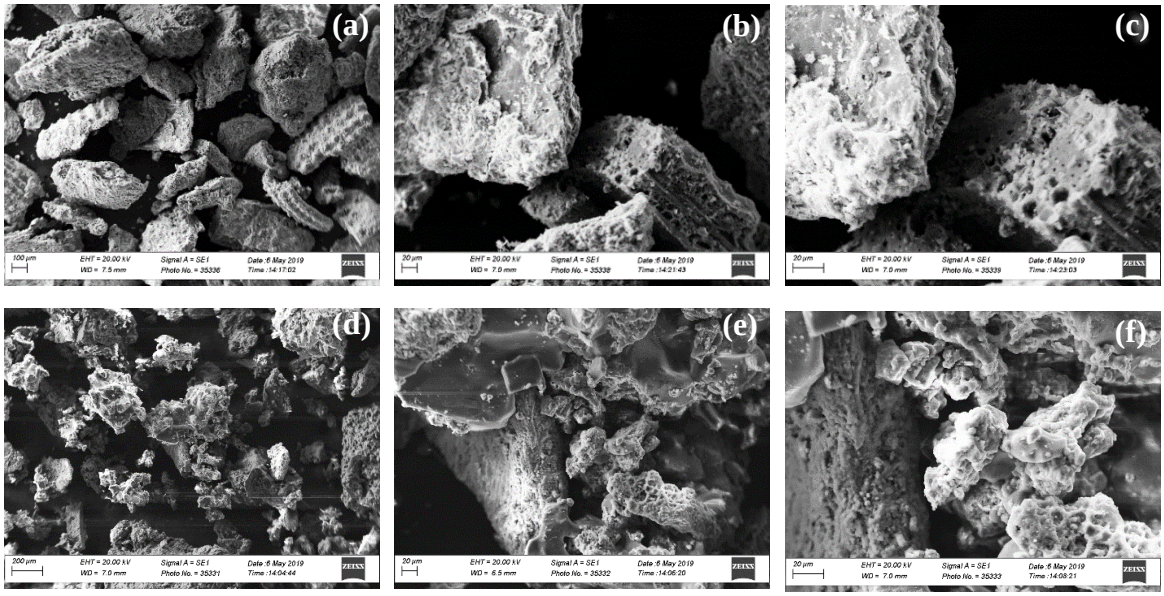

Figure 1. Scanning electron microscopy images (SEM) of BBF before and after urea impregnation. Figures a, b, and c for PLB and figures d, e, and f for PLB-N, at 100, 500, and 1000 times of increase, respectively.

Pores are formed by the decomposition of organic macromolecules and gives PLB the ability to accommodate urea molecules (Ejraei et al., 2019). Furthermore, co-pyrolysis of PL with H_3PO_4 + MgO increase surface area and small pores (Carneiro et al. 2018) that can potentially promote the link between urea and surface functional groups through chemical reaction.

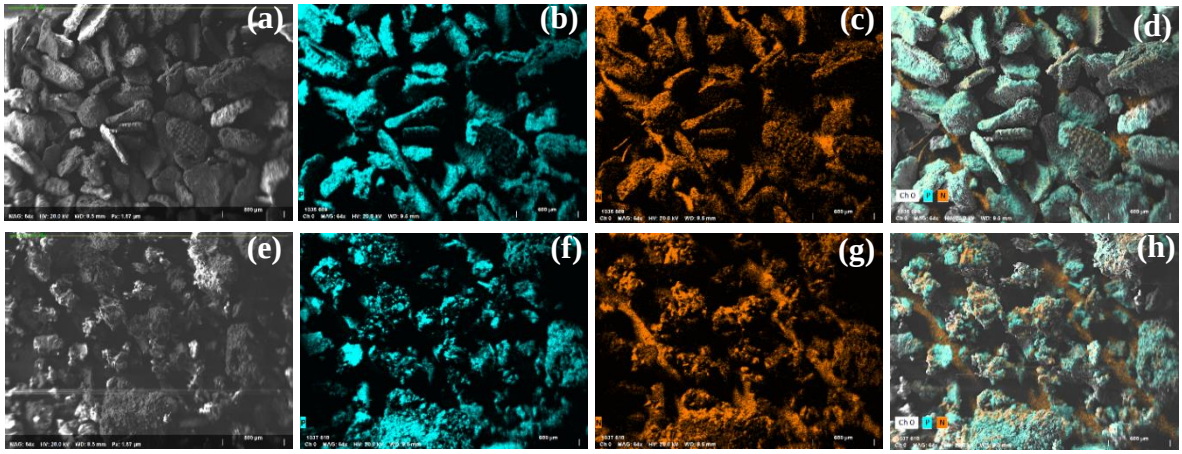

Figure 2. Energy-dispersive X-ray spectroscopy images (EDX) of BBF before and after urea impregnation of PLB (a) and PLB-N (e), SEM-EDS mapping for P (b and f), N (c and g) and NP (d and h).

The energy dispersive X-ray spectroscopy (EDS) of PLB and PLB-N confirmed that there was, potentially, an impregnation of P in pre-pyrolysis of poultry litter (Figure b and f). In fact, the comparison of the EDX spectra for PLB (Figure 2e) and PLB-N (Figure 2h and d) shows the successful impregnation of PLB with N. The FTIR results showed that urea interacted with the biochar by reactions with the BBF carboxyl and phenolic group (Figure 3). The reduced peak intensities and displaced in carboxyl and phenolic groups indicate the urea loading and the absence of other forms of N (for example NH_4^+ -N or NH_3-N) in the BBF structure.

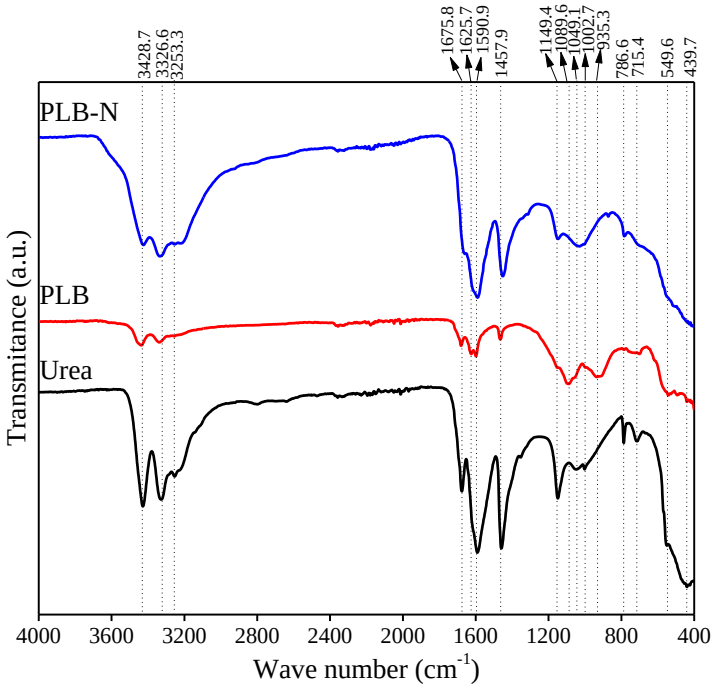

Figure 3. Fourier Transform Infrared Spectroscopy (FTIR) of urea and BBFs before (PLB) and after (PLB-N) urea impregnation.

After loading with urea, PLB-N showed the absorption bands characteristic of urea in 3428.7 to 3253.3 cm^{-1}, the doublet is characteristic of primary amides in the NH_2 group; the band in 1675.8 is characteristic of amide carbonyl; the band at 1675.8 cm^{-1} is characteristic of the amyl carbonyl; at 1625.7 cm^{-1} another common fold in primary amides is evidenced, associated with the C = O bond of the urea molecule; and in 1457.9 and 1149 cm^{-1} the bands are related to C-N axial deformation (Pavia et al. 2010).

Crop yield and nitrogen and phosphorus uptake

The shoot dry matter production (SDM) of common bean and maize is shown in Figures 4a and 4b. In the first growing cycle, significantly ($p < 0.05$) higher yields of SDM were observed for common bean fertilizer with TSP + urea when compared with the treatment of PLB-N and the control without application of N and P (Figure 4a). The response of SDM to N doses via PLB-N was best described by a quadratic model with the maximum yield obtained by the application of 100 mg kg^{-1} of N, after which there was a decrease in yield.

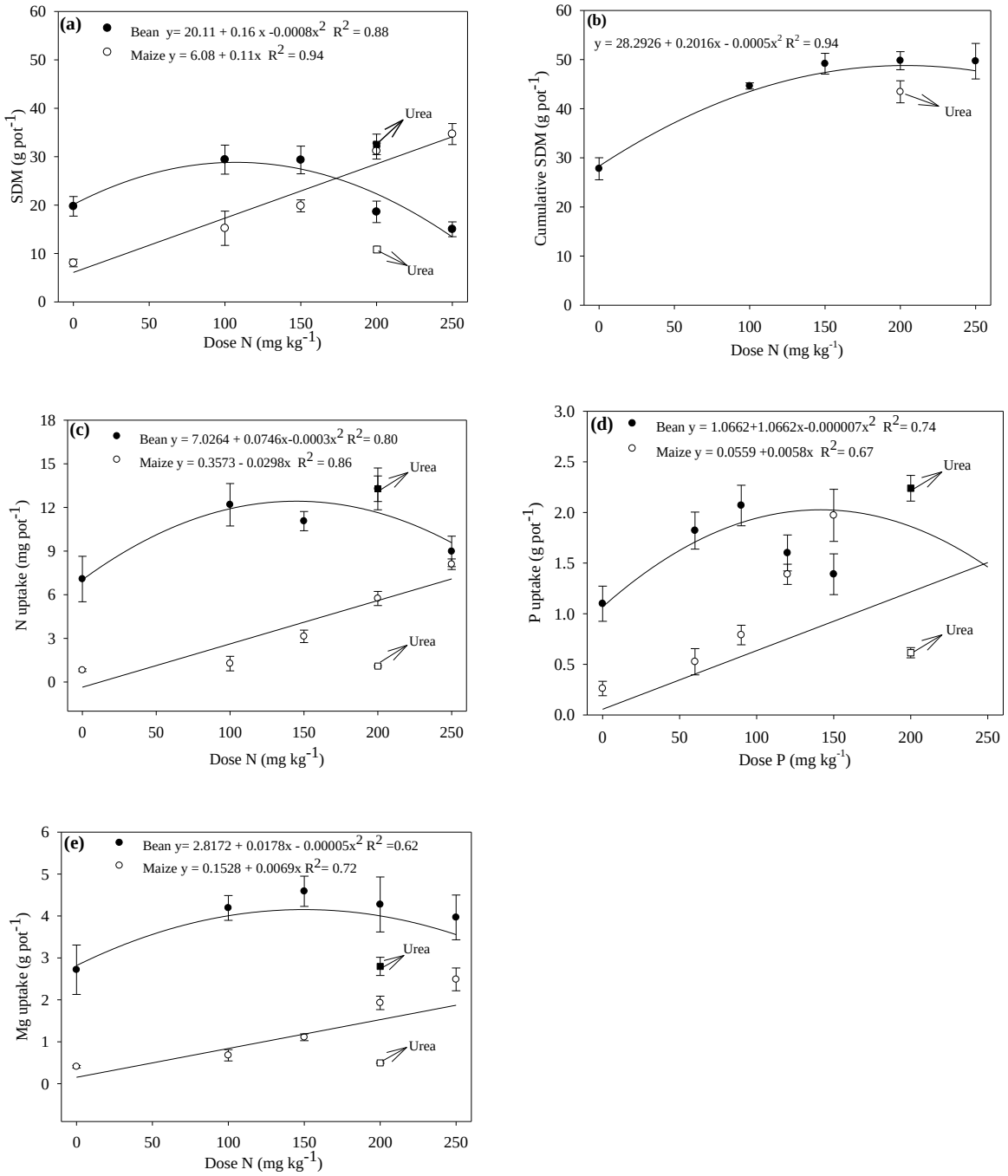

Figure 4. Shoot dry mass (SDM) of bean plants in the first crop and maize plants in the subsequent crop (a); SDM accumulation of the two crop cycles of plants under PLB-N fertilization and urea (b); uptake of N (c), P (d), and Mg (e) by the plant. Total dry mass = Σ production of dry mass of beans and maize. Error bars represent standard error.

In the second cultivation cycle, the SDM yield of maize responded linearly to the increasing doses of N ($p < 0.05$, Figure 4b). Residual N fertilization with PLB-N was able to sustain the highest yields of SDM ranging from 15 to 35 g pot^{-1} with the increase in N doses,

while urea at 200 mg kg^{-1} yielded 11 g pot^{-1} (Figure 4b). There was a much higher relative agronomic efficiency (RAE) for PLB-N 285% when compared with urea (RAE of 100%) at the same dose of N (200 mg kg^{-1}). The SDM in the control without N and P fertilization decreased significantly with the lowest yield (8 g pot^{-1}) in maize.

The decrease in yield of common bean over 100 mg kg^{-1} of N via PLB-N indicates a rapid release profile that saturates the absorption of N by the plant without any additional response in the production of SDM. The physical mixture of BBF with urea was not effective in reducing the N hydrolysis rate in PLB-N fertilizers, that resulted in a marked increase in the soil EC (Figure 4c), and delayed the germination of the common bean seedlings and caused injuries that reflected in reduced SDM productivity (Figure 3a). High concentrations of urea can compromise germination and plant growth due to toxicity caused by the high level of NH_3/NH_4^+ (Pan et al. 2016) and can also induce the salt stress provided by the high concentration of NH_4^+ and NO_2^- ions (Esteban et al. 2016).

Conversely, the residual effect of fertilization for maize was much higher for PLB-N than for urea and caused a linear response likely due to the higher N availability in the soil. Saha et al. (2019) showed that the increase in the cation exchange capacity promoted by the biochar particles prolonged the N availability from urea, which might have been the case in this study. The linear response of maize to N caused the total production of SDM (Σ production of dry mass of beans and maize) to be equal or higher in the soil treated with PLB-N in all N doses when compared with urea only (Figure 4c).

Nitrogen, P, and Mg uptake by bean plants was severely affected by the salt stress caused by the increase in N doses via PLB-N (Figures 4c, d and e). Nitrogen uptake was higher in common bean plants that received 200 mg kg^{-1} of N via PLB-N and the equivalent dose via urea. In the subsequent cultivation, N uptake by maize followed a linear trend with N doses via PLB-N ($p < 0.05$), with values ranging from 1.3 to 8.1 mg pot^{-1}, while in the treatment with conventional urea the N uptake was 1.09 mg pot^{-1}.

The higher or lower P uptake for both common bean and maize is also directly related to the availability of P (Figure 4d), which in turn is greatly influenced by the soil pH. This might explain the greater P uptake promoted by the control treatment with the application of TSP in the cultivation of common beans and the linear response to the increase in the doses of PLB-N for maize. The decrease in P uptake with the increase in the doses of PLB-N (Figure 4d) might also be related to the increase ionic strength caused by the increase in N doses applied fully at sowing. The acquisition of nutrients by plants can be interrupted by excessive ions in the

solution, either by direct ionic competition or by decreasing the osmotic potential of the solution, reducing the mass flow of mineral nutrients to the root (Fageria et al. 2011). Furthermore, the decrease in Mg uptake by bean plants (Figure 4e) can also be attributed to toxicity due to excess NH_4^+, considering that one of the chemical changes in the plant induced by excess NH_4^+ includes depression in the uptake of essential cations (as K^+, Ca^{2+} and Mg^{2+}) (Britto and Kronzucker 2002).

Soil conditions after cultivations

After the cultivation of common beans, the soil pH decreased by 0.35 to 1.36 unit due to N doses above 150 mg kg^{-1} via PLB-N when compared with control without N (Figure 5a). When comparing the soil pH of urea and PLB-N at the same N dose (200 mg kg^{-1}), it was verified a significant (p<0.05) but small difference of 0.3 unit. It must be highlighted, however, that the N dose (200 mg kg^{-1}) from urea was splitted 3 times while the same N dose via PLB-N was applied all at sowing. Soil acidification due to N addition has been also observed in other studies due to the nitrification process (Tian and Niu 2015; Hao et al. 2020).

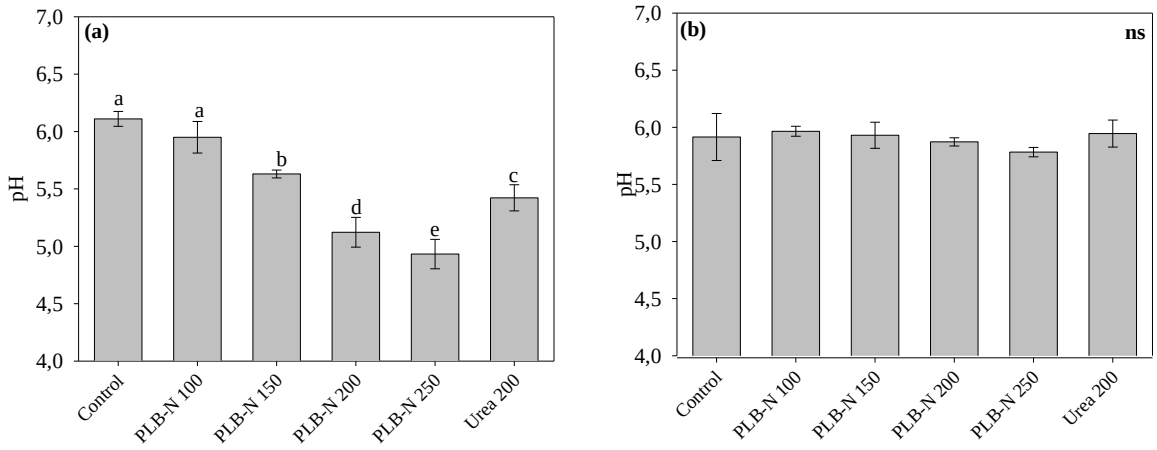

Figure 5. Soil pH after the cultivation of common beans (a) and maize (b) under PLB-N and urea fertilization. ^{ns} means not significant. Bars followed by the same letters do not differ by Scott Knott test (p *<0.05*); the error bars represent the standard error (n = 3).

Although the soil pH gradually decreased with increasing N doses after common bean cultivation, there was no significant (p < 0.05) differences among the treatments after the subsequent maize cultivation (p *<0.05*; Figure 5b), which means the soil acidification caused by the N addition was only a transient effect in the studied soil. The soil acidification was

mainly due to an increase in the rate of transformation of N, increasing the nitrification of NH_4^+ (De Vries and Breeuwsma 1987). The absorption of N-NH_4^+ by crops also contributes to soil acidification due to protons generated and released by the roots of plants to balance the excess absorption of cations and anions (Han et al. 2015). Unlike PLB-N, possibly, the impact of N transformations on soil acidification for urea was low due to splitting and the N absorption by the crop was the main driver of soil acidification (Hao et al. 2020).

Generally, in a short-term experiment, the application of BBFs impregnated with MgO promotes an increase in soil pH around the application point due to the alkaline nature of the fertilizers (Lustosa Filho et al. 2017; Lustosa Filho et al. 2019). However, the method of application, combined with the high rates of PLB-N, seems to have prevented the alkaline reaction of BBF and limited its ability to buffer the soil pH. The biochar's ability to buffer the soil pH is directly related to the CEC contained in this material (Xu et al. 2012) and may have alleviated the acidification of the soil pH.

The EC values increased significantly with the increase in N, except for the urea treatment, in which the EC was equal or lower than the treatment without N application ($p < 0.05$; Figure 6a). At the same dose of N (200 mg kg^{-1}), the difference between the EC values of the treatment with PLB-N and that of the control treatment was approximately 6.26 units. Moreover, soil EC values with PLB-N at 200 and 250 mg kg^{-1} exceeded the tolerance limit (4 dS m^{-1}) for most crops (Fageria et al. 2011). However, after maize cultivation, there was a marked decrease in soil salinity, which varied from 0.8 to 1.6 dS m^{-1} with the increase in PLB-N doses (Figure 6b).

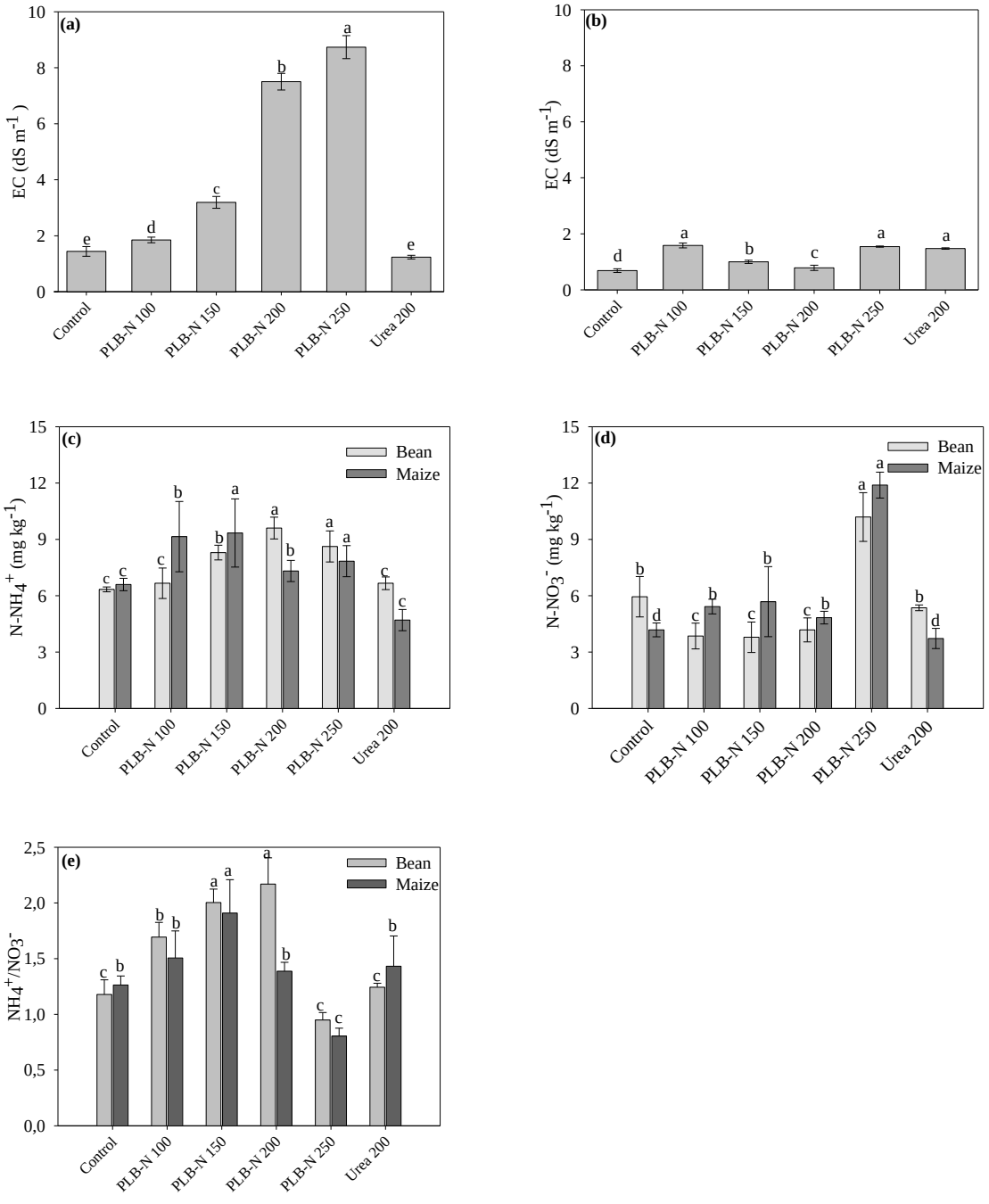

Figure 6. Electric conductivity (EC) of the soil after the cultivation of beans (a) and after the subsequent cultivation of maize (b); available NH_4^+ (c) and NO_3^- (d); NH_4^+/NO_3^- ratio (e) in the soil under PLB-N and urea fertilization; means followed by the same letters in the bars do not differ by Scott Knott test ($p < 0.05$); the error bars represent the standard error (n = 3).

The increase in soil salinity with the increase of PLB-N doses in a single application was possibly induced by an increase in the concentration of mineral N and partly by the BBFs soluble nutrients. According to the NH_4^+/NO_3^- ratio after bean cultivation (Figure 6e),

nitrification was significantly reduced with an increase in the N rate, leading to higher concentrations of NH_4^+-N and lower NO_3^--N, except for the highest N dose, which presented the lowest NH_4^+/NO_3^- ratio, suggesting an increase in nitrification, which was maintained after the cultivation of corn. Comparing the ratio NH_4^+/NO_3^- after each crop it was observed a decrease in this ratio, which was more pronounced at the dose of 200 mg kg^{-1}.

The nitrification of excess fertilizer N led to a large release of protons, and soil acidification may have further induced the direct release of basic cations (Mg^{2+} and Ca^{2+}), accelerating soil salinization (Han et al. 2015). This justifies the strategy of splitting urea fertilization to help reduce salt stress due to the high concentration of NH_4^+ from urea hydrolysis (Court et al. 1964) and reduce N losses (Cantarella 2007). The high salinity of the soil inhibits the absorption of N by the root, which explains the decline in N uptake with the increase in the doses of PLB-N (Figure 4c).

Increased soil salinity limits the yield and productivity of crops and is one of the main factors that limit the growth and productivity of common beans (Bayuelo-Jiménez et al. 2002). The stress caused by the increase in soil salinity reduces plant growth, including leaf area, which reduces the photosynthetic process and efficiency in the use of nutrients (Fageria et al. 2011). Saline stress delayed bean germination and contributed to lower SDM yield (Figure 4a).

The concentrations of mineral N in the soil are shown in Figure 6c and d. The highest levels of NH_4^+ were obtained with the application of PLB-N in the highest doses of N (200 and 250 mg kg^{-1}), while in the treatment with urea the levels were equivalent to the treatment without application of N (Figure 6c). After the cultivation of maize, the levels of NH_4^+were higher at doses of 100, 150, and 250 mg kg^{-1} of N via PLB-N ($p < 0.05$). The application of N via PLB-N in the same dose as the treatment with urea (200 mg kg^{-1}) resulted in higher levels of NH_4^+ either after the cultivation of beans and maize.

There were no significant differences between the levels of nitrate (NO_3^-) in the soil treated with the addition of N after bean cultivation (Figure 6d), except for the highest dose of N via PLB-N, which presented the highest levels of NO_3^-, both after the first and after the second cultivation cycle. When comparing the levels of NO_3^- in the soil after the cultivation of beans with the levels after the cultivation of maize, we noticed an increase in the levels of NO_3^- in the soil, only in the treatments with an application of PLB-N (Figure 6d).

Application of PLB-N kept the mineral N in the form of NH_4^+ considerably higher, which suggests the role of biochar in increasing the retention of N for a longer period and consequently the absorption by plants likely due to the high CEC of this material (Lustosa Filho

et al., 2017). The lower availability of NH_4^+ can also decrease the nitrification of NH_4^+ to NO_3^- resulting in a lower concentration of NO_3^- in the soil solution when compared with urea only (Saha et al. 2018).

The addition of PLB-N promoted a significant increase in the levels of P extractable by resin measured in the soil after bean cultivation ($p < 0.05$, Figure 7a). The magnitude of this increase was proportional to the increase in the application rate, with P levels ranging from 15 to 25.5 mg kg^{-1}, although lower than the treatment with TSP (33.7 mg kg^{-1}). This same trend was observed after the subsequent cultivation with maize (Figure 7b), however, the level of P extractable by resin in the fertilized soil with the highest rates of PLB-N, which provided 120 and 150 mg kg^{-1} of P, was lower or similar to the control treatment treated with TSP ($p < 0.05$) fertilized with 200 mg kg^{-1} of P. While in the treatments with the doses of 100 and 150 mg kg^{-1}, they were greater than or equal to the treatment without fertilization with P.

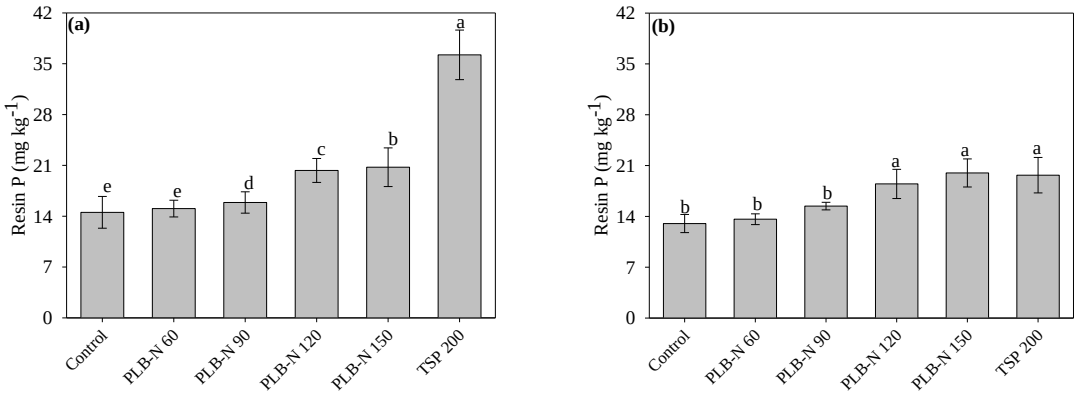

Figure 7. P resin soil levels after the cultivation of beans (a) and after the subsequent cultivation of maize (b) under PLB-N and TSP fertilization; means followed by the same letters in the bars differ by Scott Knott test ($p < 0.05$); the error bars represent the standard error.

The amount of P supplied via PLB-N, was lower than the amount of P added in the control treatment with TSP, even at the highest application rate. As our goal was to test this fertilizer as an NP source, we chose not to supplement the dose of P supplied via PLB-N with a soluble source such as TSP. At BBF, low water-soluble P (Table 2) with a slow and steady P release model (Lustosa Filho et al. 2017; Carneiro et al. 2021), may not benefit in the short term crops that require high P absorption when compared with a highly soluble P source. Probably, restricted access to P in the short term was also a limiting factor for the growth of common beans and contributed to the lowest SDM and is in line with the findings of other studies (Lustosa Filho et al. 2019; Santos et al. 2019). Despite this, the levels of P extractable by resin

in the soil fertilized with PLB-N at doses of 200 and 250 mg kg^{-1} of N, which provided between 60 and 75% of the dose of P (200 mg kg^{-1}) reached values greater than or similar to the soil fertilized with TSP. With the time of cultivation, the acidification of the rhizosphere (Freitas et al. 2013) and the acidity resulting from the urea nitrification and NH_4^+ absorption may have stimulated the solubilization of P from the PLB-N, since the impregnated BBFs with alkaline sources such as MgO, they need the acidity of the soil to be solubilized.

At first, the application of TSP ensured the greatest supply of P and SDM yield of beans, due to the high solubility of this source in water (Lustosa Filho et al. 2020). However, the amount of P that was not absorbed by plants is limited by rapid immobilization by the mineral fraction rich in iron (Fe) and aluminum (Al) oxides and hydroxides in tropical soils (Abdala et al. 2018).

Conclusions

In the present study, we investigated the effect of increasing doses of biochar-based phosphate fertilizer enriched with urea, applied at once at sowing, in the absorption of N and P in the cultivation of beans followed by maize, in comparison with conventional fertilization with urea (split) and a soluble phosphate (TSP). The results showed that the NP fertilizer based on biochar did not delay the release of N, but affected the predominance of mineral N in the form of NH_4^+ in the soil. The main effect of PLB-N was the residual fertilization, demonstrating biochar-based phosphate fertilizers have potential as a support material to increase the availability and efficiency of N use by plants. However, for the application of the dose at once it is necessary to control the rate of N release through granulation or peletization. This control of N release will allow the application of the total dose in the furrow, without the need for installments, which will facilitate the cultural management of the crop. Future studies should be the focus on understanding in more detail the role of engineered biochar-based phosphate fertilizers as a urea transporter and the effect of its interaction with various soil types on the dynamics and mineralization of N. Therefore, incubation studies to assess retention of N from the fertilizer in the soil, the gaseous emissions, and the leaching of N must be conducted.

Acknowledgements

This work was financially supported by the National Council for Scientific and Technological Development (CNPq – Grant Nº 404076/2016-5). Coordination for the Improvement of Higher Education Personnel (CAPES/PROEX) and Foundation for Research of the State of Minas

Gerais (FAPEMIG) also financially supported this work. LCA Melo is a research fellow of the National Council for Scientific and Technological Development (CNPq – Grant Nº 308943/2018-0). The authors would like to thank the Laboratory of Electron Microscopy and analysis of Ultrastructural Federal University of Lavras, and Finep, Fapemig, CNPq e Capes for supplying the equipment and technical support for experiments involving electron microscopy.

References

Abdala DB, Moore PA, Rodrigues M, Herrera WF, Pavinato PS. 2018. Long-term effects of alum-treated litter, untreated litter and NH_4NO_3 application on phosphorus speciation, distribution and reactivity in soils using K-edge XANES and chemical fractionation. J Environ Manage [Internet].

Bayuelo-Jiménez JS, Craig R, Lynch JP. 2002. Salinity tolerance of Phaseolus species during germination and early seedling growth. Crop Sci. 42(5):1584–1594.

Bindraban PS, Dimkpa CO, White JC, Franklin FA, Melse-Boonstra A, Koele N, Pandey R, Rodenburg J, Senthilkumar K, Demokritou P, Schmidt S. 2020. Safeguarding human and planetary health demands a fertilizer sector transformation. Plants, People, Planet. 2(4):302–309.

Bowles TM, Atallah SS, Campbell EE, Gaudin ACM, Wieder WR, Grandy AS. 2018. Addressing agricultural nitrogen losses in a changing climate. Nat Sustain [Internet]. 1(8):399–408. http://dx.doi.org/10.1038/s41893-018-0106-0.

Brasil. 2017. Manual de métodos analíticos oficiais para fertilizantes e corretivos. Brasilia - DF: MAPA, Ministério da Agricultura Pecuária e Abastecimento/SDA, Secretaria de Defesa Agropecuária.

Bremner JM, Mulvaney CS. 1982. Methods of soil analysis. In: Miller RH, Keeney DR, editors. Madison: A. [place unknown]; p. 595–624.

Britto DT, Kronzucker H. J. 2002. Review NH4+ toxicity in higher plants: a critical review I . Introduction. 584(3).

Cantarella H. 2007. Nitrogênio. In: Novais R., Alvarez VH, Barros NF, Fontes RL., Cantarutti RB, Neves JCL, editors. Fertil do Solo. SBCS. Viçosa, MG; p. 375–470.

Cantarella H, Trivelin PO. 2001. Determinacaõ de nitrogênio inorgânico em solo pelo método da destilação a vapor In Análise química para avaliação da fertilidade de solos tropicais. (January).

Carneiro JS da S, Ribeiro ICA, Nardis BO, Barbosa CF, Lustosa Filho JF, Melo LCA. 2021. Long-term effect of biochar-based fertilizers application in tropical soil: Agronomic efficiency

and phosphorus availability. Sci Total Environ [Internet]. 760:143955. https://doi.org/10.1016/j.scitotenv.2020.143955.

Carneiro JSDS, Lustosa Filho JF, Nardis BO, Ribeiro-Soares J, Zinn YL, Melo LCA. 2018. Carbon Stability of Engineered Biochar-Based Phosphate Fertilizers. ACS Sustain Chem Eng. 6(11):14203–14212.

Chen L, Chen XL, Zhou CH, Yang HM, Ji SF, Tong DS, Zhong ZK, Yu WH, Chu MQ. 2017. Environmental-friendly montmorillonite-biochar composites: Facile production and tunable adsorption-release of ammonium and phosphate. J Clean Prod [Internet]. 156:648–659. http://dx.doi.org/10.1016/j.jclepro.2017.04.050.

Court MN, Stephen C, Waidj JS. 1964. Toxicity as a cause of the inefficiency of urea as a fertilizer. Journal of Soil Science. Vol. 15. No. 1. 1964.

Ejraei A, Aroon MA, Ziarati Saravani A. 2019. Wastewater treatment using a hybrid system combining adsorption, photocatalytic degradation and membrane filtration processes. J Water Process Eng, https://doi.org/10.1016/j.jwpe.2019.01.003.

Enders A, Hanley K, Whitman T, Joseph S, Lehmann J. 2012. Characterization of biochars to evaluate recalcitrance and agronomic performance. Bioresour Technol [Internet]. 114:644–653. http://dx.doi.org/10.1016/j.biortech.2012.03.022.

Erisman JW, Sutton MA, Galloway J, Klimont Z, Winiwarter W. 2008. How a century of ammonia synthesis changed the world. Nat Geosci.

Esteban R, Ariz I, Cruz C, Moran JF. 2016. Review: Mechanisms of ammonium toxicity and the quest for tolerance. Plant Sci [Internet]. http://dx.doi.org/10.1016/j.plantsci.2016.04.008

Fageria NK, Baligar VC. 2005. Enhancing Nitrogen Use Efficiency in Crop Plants. Adv Agron. 88(05):97–185.

Fageria NK, Gheyi HR, Moreira A. 2011. Nutrient bioavailability in salt affected soils. J Plant Nutr. 34(7):945–962.

Ferreira DF. 2014. Sisvar : A Guide for Its Bootstrap Procedures in Multiple Comparisons Sisvar : um guia dos seus procedimentos de comparações múltiplas Bootstrap. Ciência e Agrotecnologia. 38(2):109–112.

Freitas IF de, Novais RF, Villani EM de A, Novais SV. 2013. Phosphorus extracted by ion exchange resins and Mehlich-1 from oxisols (latosols) treated with different phosphorus rates and sources for varied soil-source contact periods. Revista Brasileira de Ciência do Solo. 37(3):667–677.

González ME, Cea M, Medina J, González A, Diez MC, Cartes P, Monreal C, Navia R. 2015. Evaluation of biodegradable polymers as encapsulating agents for the development of a urea controlled-release fertilizer using biochar as support material. Sci Total Environ [Internet]. [accessed 2018 Dec 17] 505:446–453. https://www.sciencedirect.com/science/article/pii/S0048969714014521.

Gwenzi W, Nyambishi TJ, Chaukura N, Mapope N. 2018. Synthesis and nutrient release patterns of a biochar-based N–P–K slow-release fertilizer. Int J Environ Sci Technol. 15(2):405–414.

Han J, Shi J, Zeng L, Xu J, Wu L. 2015. Effects of nitrogen fertilization on the acidity and salinity of greenhouse soils. Environ Sci Pollut Res. 22(4):2976–2986.

Hao T, Zhu Q, Zeng M, Shen J, Shi X, Liu X, Zhang F, de Vries W. 2020. Impacts of nitrogen fertilizer type and application rate on soil acidification rate under a wheat-maize double cropping system. J Environ Manage [Internet]. 270(May):110888. https://doi.org/10.1016/j.jenvman.2020.110888.

Lehmann J, Joseph S. 2015. Biochar for environmental management: science, technology and implementation. Earthscan, New York.

Leite A de A, Cardoso AA de S, Leite R de A, Oliveira-Longatti SM de, Lustosa Filho JF, Moreira FM de S, Melo LCA. 2020. Selected bacterial strains enhance phosphorus availability from biochar-based rock phosphate fertilizer. Ann Microbiol. 70(6):1–13.

Li R, Wang JJ, Zhang Z, Awasthi MK, Du D, Dang P, Huang Q, Zhang Y, Wang L. 2018. Recovery of phosphate and dissolved organic matter from aqueous solution using a novel CaO-MgO hybrid carbon composite and its feasibility in phosphorus recycling. Sci Total Environ [Internet]. 642:526–536. https://doi.org/10.1016/j.scitotenv.2018.06.092

Lu C, Tian H. 2017. Global nitrogen and phosphorus fertilizer use for agriculture production in the past half century: Shifted hot spots and nutrient imbalance. Earth Syst Sci Data. 9(1):181–192.

Lustosa Filho J. F, Carneiro JSDS, Barbosa CF, Lima KP, Leite A do A, Melo L carrijo. A, Melo A. 2020. Science of the Total Environment Aging of biochar-based fertilizers in soil : Effects on phosphorus pools and availability to *Urochloa brizantha* grass. Sci Total Environ [Internet]. 709:136028. https://doi.org/10.1016/j.scitotenv.2019.136028.

Lustosa Filho JF, Barbosa CF, Carneiro JS da S, Melo LCA. 2019. Diffusion and phosphorus solubility of biochar-based fertilizer: Visualization, chemical assessment and availability to plants. Soil Tillage Res [Internet]. 194(October 2018):104298. https://doi.org/10.1016/j.still.2019.104298.

Lustosa Filho JF, Penido ES, Castro P, Silva CA, Melo LCA. 2017. Co-Pyrolysis of Poultry Litter and Phosphate and Magnesium Generates Alternative Slow-Release Fertilizer Suitable for Tropical Soils.

Malavolta E, Vitti GC, Oliveira SA. 1997. Avaliação do estado nutricional das plantas - Princípios e aplicações. 2nd ed. Piracicaba, SP: Associação Brasileira para Pesquisa da Potassa e do Fósforo.

Murphy J, Riley JP. 1962. A modified single solution method for the determination of phosphate in natural waters. Anal Chim Acta [Internet]. [accessed 2019 May 15] 27:31–36. https://www.sciencedirect.com/science/article/pii/S0003267000884445.

Nardis BO, Santana Da Silva Carneiro J, Souza IMG De, Barros RG De, Azevedo Melo LC. 2020. Phosphorus recovery using magnesium-enriched biochar and its potential use as fertilizer. Arch Agron Soil Sci [Internet]. 00(00):1–17. https://doi.org/10.1080/03650340.2020.1771699

Novais RF, Smyth TJ. 1999. Fósforo em solo e planta em condições tropicais. Informações Agronômicas. 87:10–11.

Novais RF, Neves JCL, Barros NF. 1991. Ensaio em ambiente controlado. In: Oliveira AJ, Garrido WE, Araújo JD, Lourenço S, editors. Métodos de Pesquisa em Fertilidade do solo. Brasília: Embrapa-SEA; p. 189–253.

Pan WL, Madsen IJ, Bolton RP, Graves L, Sistrunk T. 2016. Ammonia/ammonium toxicity root symptoms induced by inorganic and organic fertilizers and placement. Agron J. 108(6):2485–2492.

Pavia DL, Lampman Gm, Kriz GS, Vyvyan JR. 2010. Introdução à espectroscopia. 4th ed. Learning C, editor. São Paulo.

Puga AP, Queiroz MC de A, Ligo MAV, Carvalho CS, Pires AMM, Marcatto J de OS, Andrade CA. 2019. Nitrogen availability and ammonia volatilization in biochar-based fertilizers. Arch Agron Soil Sci. 0340.

Raij B van, Quaggio JA, Silva NM da. 1986. Extraction of phosphorus, potassium, calcium, and magnesium from soils by an ion-exchange resin procedure. Commun Soil Sci Plant Anal. 17(5):547–566.

Rajkovich S, Enders A, Hanley K, Hyland C, Zimmerman AR, Lehmann J. 2012. Corn growth and nitrogen nutrition after additions of biochars with varying properties to a temperate soil. Biol Fertil Soils [Internet]. [accessed 2018 May 21] 48(3):271–284. http://link.springer.com/10.1007/s00374-011-0624-7.

Saha BK, Rose MT, Wong VNL, Cavagnaro TR, Patti AF. 2018. Nitrogen Dynamics in Soil Fertilized with Slow Release Brown Coal-Urea Fertilizers. Sci Rep. 8(1):1–10.

Santos SR, Filho JFL, Vergütz L, Melo LCA. 2019. Biochar association with phosphate fertilizer and its influence on phosphorus use efficiency by maize. Cienc e Agrotecnologia. 43.

Shi W, Ju Y, Bian R, Li L, Joseph S, Mitchell DRG, Munroe P, Taherymoosavi S, Pan G. 2020. Science of the Total Environment Biochar bound urea boosts plant growth and reduces nitrogen leaching. Sci Total Environ [Internet]. 701:134424. https://doi.org/10.1016/j.scitotenv.2019.134424.

Silva FC. 2009. Manual de análises químicas de solos, plantas e fertilizantes. 2nd ed. Silva FC, editor. Brasília, DF: Empresa Brasileira de Pesquisa Agropecuária, Embrapa Solos.

Tian D, Niu S. 2015. A global analysis of soil acidification caused by nitrogen addition. Environ Res Lett. 10(2).

Trenkel. 2013. Slow and Controlled-Release and stabilized Fertilizers. [place unknown].

De Vries W, Breeuwsma A. 1987. The relation between soil acidification and element cycling. Water Air Soil Pollut. 35(3–4):293–310.

Wen P, Wu Z, Han Y, Cravotto G, Wang J, Ye BC. 2017. Microwave-Assisted Synthesis of a Novel Biochar-Based Slow-Release Nitrogen Fertilizer with Enhanced Water-Retention Capacity. ACS Sustain Chem Eng. 5(8):7374–7382.

Xu R Kou, Zhao A Zhen, Yuan J Hua, Jiang J. 2012. pH buffering capacity of acid soils from tropical and subtropical regions of China as influenced by incorporation of crop straw biochars. J Soils Sediments. 12(4):494–502.

Zhang X, Davidson EA, Mauzerall DL, Searchinger TD, Dumas P, Shen Y. 2015. Managing nitrogen for sustainable development. Nature [Internet]. 528(7580):51–59. http://dx.doi.org/10.1038/nature15743.

Zhao, L., Cao, X., Zheng, W., Scott, J.W., Sharma, B.K., Chen, X., 2016. Co-Pyrolysis of Biomass with Phosphate Fertilizers to Improve Biochar Carbon Retention, Slow Nutrient Release , and Stabilize Heavy Metals in Soil. ACS Sustain. Chem. Eng. 1630−1636. https://doi.org/https://doi.org/10.1021/acssuschemeng.5b01570.

CONCLUDING REMARKS

The BBFs enriched with MgO are slow-release sources of P suitable for a growth culture that does not require high levels of P in the very short-term and can effectively contribute to the construction of soil nutrients repository. This is particularly beneficial for highly weathered tropical soils and reveals the real potential of these BBFs, which have increased the P use efficiency over a conventional p source (TSP) and an organomineral phosphate fertilizer. Interesting aspects were observed when combining the coffee growth results with the chemical fractions of P. Firstly, the P species identified by sequential extraction showed trends consistent with the P species identified by P K-edge XANES spectroscopic analysis. However, the sequential chemical fractions of P did not effectively reflect the bioavailability of P from BBFs in the soil and showed the importance of validating the results obtained in the sequential fractionation of fertilizers with bioavailability tests. Thus, we were able with this work to demonstrate that BBFs enriched with MgO can increase the efficiency of use of P in an Oxisol in the medium- and long-term and contribute to the increase of the labile and moderately labile fractions of P after cultivation. These findings are central to the development of criteria to identify situations in which BBF can be used effectively and economically feasible for farmers.

The loading of poultry litter biochar enriched with phosphoric acid and MgO with urea did not generate a slow-release NP fertilizer for its use in a single application to the soil. Despite this, we observed that the biochar has the potential as a loading matrix to preserve the availability of N and increase the residual effect and efficiency of the use of N by plants. The mechanisms that govern this process must be further evaluated to design N fertilizers more efficiently. The granulation or use of agents that slow the release of N is another aspect that should be studied as a means of controlling the release of N and for large-scale application, considering that powdered fertilizers are impractical for application in the fertilizer distribution system used in many farms. A balance must be found between controlling the release of N by minimally interfering with the effectiveness of the fertilizer as a source of P. Finally, the response of a soil-plant system to biochar-based fertilizers should be explored in more detail with field experiments, to achieve practical benefits in addition to assessing economic viability and increasing interest in the fertilizer market.